



Hybrid heart valves with VEGF-loaded zwitterionic hydrogel coating for improved anti-calcification and re-endothelialization



Qi Tong^{a,1}, Ao Sun^{b,1}, Zhengjie Wang^a, Tao Li^a, Xinye He^b, Yongjun Qian^{a,**}, Zhiyong Qian^{b,*}

^a Department of Cardiovascular Surgery, National Clinical Research Center for Geriatrics, West China Hospital, Sichuan University, Chengdu, 610041, Sichuan, PR China

^b State Key Laboratory of Biotherapy, State Key Laboratory and Collaborative Innovation Center of Biotherapy, West China Hospital, Sichuan University, Chengdu, 610041, Sichuan, PR China

ARTICLE INFO

Keywords:

Zwitterionic hydrogel
Hybrid heart valve
Anti-Calcification
Re-endothelialization
Biocompatibility

ABSTRACT

With the aging of the population in worldwide, valvular heart disease has become one of the most prominent life-threatening diseases in human health, and heart valve replacement surgery is one of the therapeutic methods for valvular heart disease. Currently, commercial bioprosthetic heart valves (BHVs) for clinical application are prepared with xenograft heart valves or pericardium crosslinked by glutaraldehyde. Due to the residual cell toxicity from glutaraldehyde, heterologous antigens, and immune response, there are still some drawbacks related to the limited lifespan of bioprosthetic heart valves, such as thrombosis, calcification, degeneration, and defectiveness of re-endothelialization. Therefore, the problems of calcification, defectiveness of re-endothelialization, and poor biocompatibility from the use of bioprosthetic heart valve need to be solved. In this study, hydrogel hybrid heart valves with improved anti-calcification and re-endothelialization were prepared by taking decellularized porcine heart valves as scaffolds following grafting with double bonds. Then, the anti-biofouling zwitterionic monomers 2-methacryloyloxyethyl phosphorylcholine (MPC) and vascular endothelial growth factor (VEGF) were utilized to obtain a hydrogel-coated hybrid heart valve (PEGDA-MPC-DHVs@VEGF). The results showed that fewer platelets and thrombi were observed on the surface of the PEGDA-MPC-DHVs@VEGF. Additionally, the PEGDA-MPC-DHVs@VEGF exhibited excellent collagen stability, biocompatibility and re-endothelialization potential. Moreover, less calcification deposition and a lower immune response were observed in the PEGDA-MPC-DHVs@VEGF compared to the glutaraldehyde-crosslinked DHVs (Glu-DHVs) after subcutaneous implantation in rats for 30 days. These studies demonstrated that the strategy of zwitterionic hydrogels loaded with VEGF may be an effective approach to improving the biocompatibility, anti-calcification and re-endothelialization of bioprosthetic heart valves.

1. Introduction

Currently, valvular heart disease is a life-threatening disease which places a huge economic burden on humans, especially elderly people. For the people with severe valvular heart disease, heart valve replacement is still an effective and commonly accepted therapeutic method. According to the statistics, more than 300,000 people with valvular heart disease have undergone heart valve replacement surgeries each year and the number is expected to triple by 2050 [1]. Therefore, the large demand for ideal artificial heart valves has become a crucial problem within the

healthcare industry.

With the development of science and technology, artificial heart valves have made great progress, and several types of artificial heart valves have been established since the first heart valve replacement was performed in 1952 [2]. Currently, the artificial heart valves used for replacement are mechanical heart valves and bioprosthetic heart valves. Although mechanical heart valves exhibit excellent mechanical properties and durability, anticoagulation therapy for people with mechanical heart valve replacement is lifelong, and the complications such as thrombogenesis and hemorrhages are still inevitable [3,4]. Bioprosthetic

* Corresponding author. State Key Laboratory of Biotherapy, State Key Laboratory and Collaborative Innovation Center of Biotherapy, West China Hospital, Sichuan University, Chengdu, 610041, Sichuan, PR China

** Corresponding author. Department of Cardiovascular Surgery, National Clinical Research Center for Geriatrics, West China Hospital, Sichuan University, Chengdu, 610041, Sichuan, PR China.

E-mail addresses: qianyongjun@scu.edu.cn (Y. Qian), anderson-qian@163.com (Z. Qian).

¹ These authors contribute equally to this work.

heart valves are made from xenograft heart valves or pericardium treated with glutaraldehyde. Bioprosthetic heart valves exhibit some advantages over mechanical heart valves, such as freedom from lifelong anti-coagulation therapy and good biocompatibility [3,4]. However, the drawbacks of bioprosthetic heart valves, such as thrombus, calcification, structural degeneration, and immune response have limited their durability [5,6]. The incidence of subclinical thrombus on interventional artificial heart valves was reported to be nearly 10–15% after 1–3 months of implantation, which is associated with an increased risk of stroke [7, 8]. Additionally, instability of the extracellular matrix (ECM) and calcification have been recognized as being associated with structural degeneration and dysfunction of the bioprosthetic heart valve [9,10]. On the other hand, calcification and the immune response have been reported to be related to the exposure of antigen epitopes and nucleation sites after structural degeneration [11]. The bioprosthetic heart valve is usually maintained for 10–15 years after implantation and cannot meet clinical demand ideally, especially for young patients who undergo heart valve replacement [12,13]. Therefore, the ideal heart valve should mimic the structure of the native heart valve, with excellent biocompatibility, anti-calcification and re-endothelialization.

Calcification, degradation and poor re-endothelialization are the main reasons for the limitations of the long-term implantation of bioprosthetic heart valves into the human body [6]. Several strategies in previous studies have been applied to overcome these drawbacks. Decellularization, referring to the removal of cells from the valves, has been shown to be an anti-calcification method [14,15]. Crosslinking is a way of improving the mechanical properties of collagens. Glutaraldehyde is used as a crosslinker to stabilize collagen, but the toxicity of the aldehyde groups can lead to poor endothelialization and residual aldehyde groups and impairing charges balances after glutaraldehyde treatment have been shown to be involved in the calcification of the bioprosthetic heart valve [11,16–18]. Some studies have reported that non-glutaraldehyde crosslinking agents such as epoxy chitosan [19], riboflavin [20], N-(3-Dimethylaminopropyl)-N'-ethylcarbodiimide hydrochloride (EDC) and N-hydroxysuccinimide (NHS) [14] have been used for the anti-calcification treatment of heart valves. Although good results have been achieved, good blood biocompatibility cannot be guaranteed. In recent years, multifunctional hydrogels have exhibited great potential in cardiac tissue engineering and hydrophilic and anti-fouling hydrogels have been developed and applied to improve the properties of bioprosthetic heart valves [21–23]. They exhibit excellent anti-biofouling and anti-calcification properties. Anti-biofouling refers to the ability of materials to resist the aggregation of proteins and microorganisms on the surface of materials. This ability is required and crucial for the implanted heart valves. The application of hydrophilic polymers such as poly (ethylene glycol) diacrylate (PEGDA) and [2-(methacryloyloxy)ethyl]dimethyl-(3-sulfopropyl) ammonium hydroxide (SBMA) to the bioprosthetic heart valve improves its antifouling and anti-calcification properties [22,24].

The endothelial cell layer plays an essential role in the long-term stability of artificial valve stents due to its antithrombotic and anti-degenerative abilities [25,26]. Currently, the toxicity of residual aldehyde groups from commercial glutaraldehyde-crosslinked bioprosthetic heart valves leads to poor re-endothelialization. Although coating with hydrophilic and anti-biofouling hydrogels can improve the biocompatibility and anti-calcification of artificial heart valves, few endothelial cells adhere to the surface due to the nonspecific anti-biofouling property. Therefore, strategies of grafting cell affinity peptides or loading VEGF might promote re-endothelialization. VEGF is known to promote the adhesion and proliferation of endothelial cells. In our study we combined hydrophilic materials, including PEGDA and 2-methacryloyloxyethyl phosphorylcholine (MPC), with vascular endothelial growth factor (VEGF) to develop hydrogel-coated hybrid heart valves. As shown in Fig. 1, fresh porcine heart valves were decellularized and then treated with methacrylic anhydride to introduce vinyl groups. The obtained heart valve (MADHVs) functioned as a double bond supplier for the

hydrogel. Then, an anti-biofouling hydrogel film loaded with VEGF was coated onto the surface of the MADHVs through photoinitiated free radical polymerization. The obtained hydrogel-coated hybrid heart valve (PEGDA-MPC-DHVs@VEGF) exhibited excellent anti-calcification, good biocompatibility and rapid re-endothelialization.

2. Materials and methods

2.1. Materials

Fresh porcine hearts were purchased from a local slaughterhouse. The porcine heart valves were harvested from the hearts and rinsed with sterilized PBS to remove blood and contaminants. Then they were stored in sterilized PBS (containing 100 U/mL penicillin and 100 µg/mL streptomycin) at 4 °C for further processing.

The poly (ethylene glycol) diacrylate (PEGDA, Mw = 1000 kDa), 2-methacryloyloxyethyl phosphorylcholine (MPC), and methacrylic anhydride were purchased from Aladdin Corp. (Shanghai, China). The lithium phenyl(2,4,6-trimethylbenzoyl) phosphinate (LAP) was purchased from Sigma-Aldrich (Shanghai, China). The recombinant human vascular endothelial growth factor (VEGF) was purchased from PERPROTECH Corp. (Shanghai, China). The Lactate-dehydrogenase (LDH) Assay Kit, collagenase I, DAPI, Triton X-100, sodium dodecyl sulfate (SDS), and ninhydrin were purchased from Solarbio Biotechnology (Beijing, China). The sodium citrate, 25% glutaraldehyde and ethanol (analytical grade) were purchased from Sinopharm Chemical Reagents Corp. (Shanghai, China). The tetra-methylrhodamine (TRITC)-phalloidin was purchased from US EVERBRIGHT INC (Suzhou, China), and a live/dead cell staining kit was purchased from KeyGen Biotech. The 4% paraformaldehyde was purchased from Biosharp Life Science Corp. (Hefei, China). A Cell Counting Kit (CCK-8) was purchased from Japan Tongren. The Human VEGF ELISA kit was purchased from Mukti Science (Hangzhou, China). The DMEM and phosphate-buffered saline (PBS, pH = 7.4) were purchased from KeyGEN Biotech (Nanjing, China).

2.2. Decellularization

The porcine bioprosthetic heart valves from porcine (PHVs) were decellularized according to the previous studies with few changes [27]. In a brief, the obtained porcine heart valves were treated with 1% Triton X-100 for 24 h at 37 °C with continuous shaking. After being rinsed in PBS three times, the heart valves were transferred to 1% SDS for another 1 h at 37 °C, followed by washing with sterilized PBS three times or more. Finally, the obtained valve samples (DHV) were preserved in sterilized PBS (containing 100 U/mL penicillin and 100 µg/mL streptomycin) at 4 °C for further experiments.

2.3. Preparation and characterization of methacrylic anhydride-modified decellularized heart valves

The methacrylic anhydride modified decellularized heart valves (MADHVs) were developed according to the previous research [28]. The DHVs were blotted dry and weighed before immersion in deionized water at a concentration of 0.1 g DHVs per 1 mL of deionized water. Methacrylic anhydride (MA) was then added dropwise into the solution at 4 °C with vigorous stirring. Then, an aqueous solution of sodium hydroxide (2 M) was dropped into the solution to maintain a pH of 7. The reaction continued at room temperature for 24 h. MADHV-0.1, MADHV-0.5, MADHV-1.0, and MADHV-3.0 refer to feed weight ratios (MA: DHVs, v/w) of 0.1, 0.5, 1.0, and 3.0, respectively. Then, the MADHVs were washed thoroughly with aqueous 50% alcohol and then deionized water three times or more.

The remaining amino groups were detected by the ninhydrin assay according to a previous study [29]. Briefly, the heart valve samples of each group were cut into 5 mm × 5 mm pieces and then placed into a small centrifuge tube, followed by the addition of 1 mL of ninhydrin

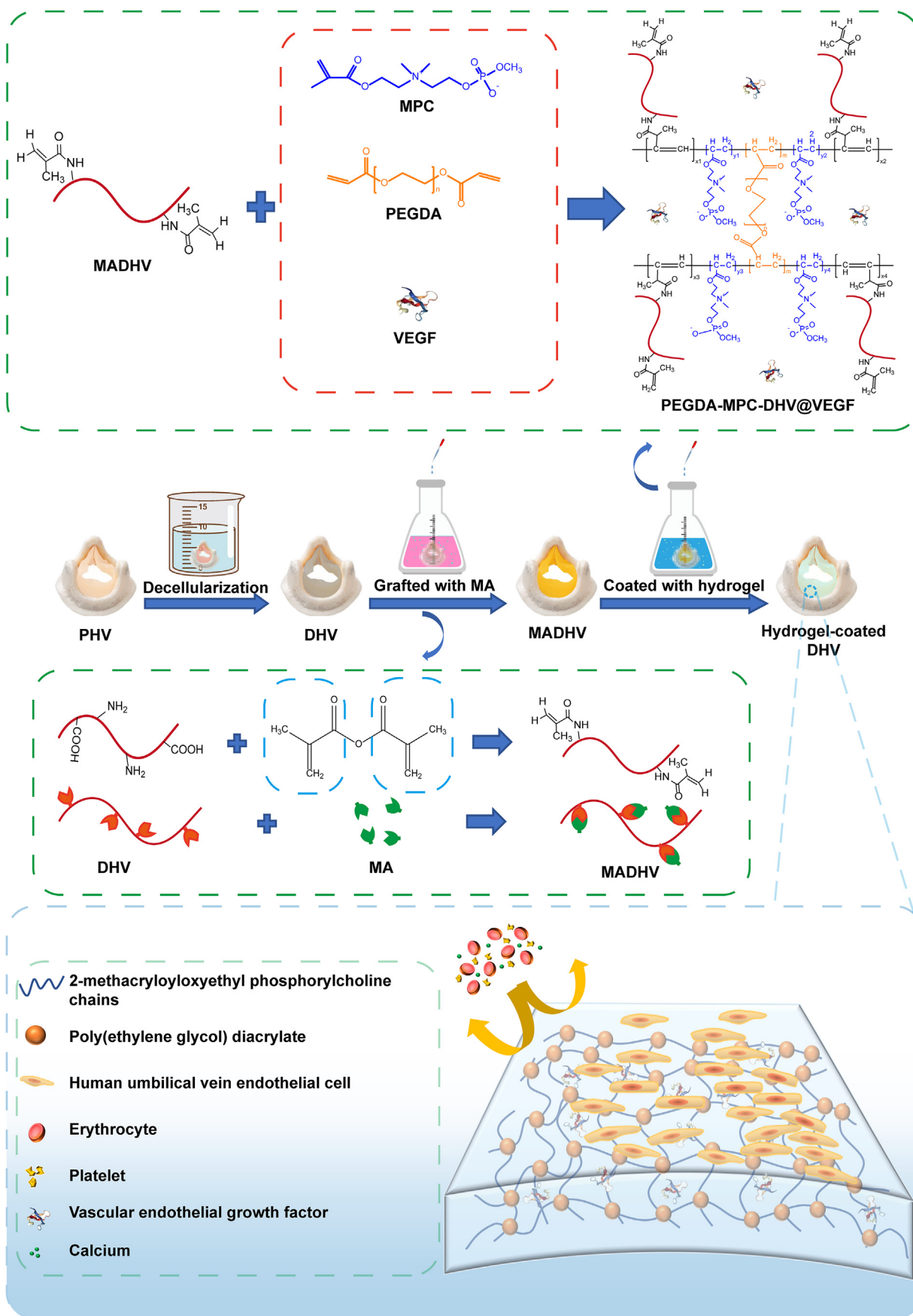


Fig. 1. Schematic preparation of the hydrogel-coated prosthetic heart valves and the microstructure of hydrogel on the PEGDA-MPC-DHV@VEGF.

solution (ethylene glycol solution with 4% ninhydrin was mixed with an equal volume of 0.2 M citrate acid solution containing 0.16% Tin chloride, pH = 5). Then, the solutions were diluted to 2 mL with deionized water. The tubes were kept in a water bath at 95 °C for 45 min. After the solution had cooled down, 250 μ L of isopropanol was added to each tube to terminate the reaction before the 200 μ L of supernatant was transferred into 96-well plates, and the OD values at 570 nm were detected by a microplate reader (Multiskan MK3, Thermo Fisher, USA). The heart valves were lyophilized and weighed. The remnant amino group content was calculated with the following formula:

$$\text{Remnant amino groups} = \frac{\text{OD}_{\text{sample}}/\text{W}_{\text{sample}}}{\text{OD}_{\text{DHV}}/\text{W}_{\text{DHV}}}$$

The DHV and MADHV samples were washed and transferred into centrifuge tubes before 0.5 mL concentrated HCl was added to each tube to dissolve the samples for 24 h at 37 °C. The supernatant was collected and dried in a vacuum oven. The obtained dried pellet was dissolved in D₂O for ¹HNMR (Varian 400).

2.4. Preparation of hydrogel-coated hybrid heart valves

Glu-DHVs: The DHVs were cross-linked with the 0.625% glutaraldehyde solution (diluted with PBS) for 24 h at 37 °C. The samples were further washed with PBS for at least three times.

PEGDA-DHVs: MADHVs were lyophilized and then immersed into the hydrogel precursor solution (15% PEGDA and initiator 0.06% LAP, w/v) for 2 h at 37 °C. Then, the samples were spread out, and 30 μ L of hydrogel precursor solution was added to the surface. The hydrogel precursor was irradiated by a visible light source (405 nm, 60 mW/cm²) for 2 min. Then, the samples were turned, and the above procedures were performed again.

PEGDA-MPC-DHVs: The lyophilized MADHVs were immersed into the hydrogel precursor solution (15% PEGDA, 15% MPC, and initiator 0.06% LAP, w/v) for 2 h at 37 °C and then were prepared as mentioned above.

PEGDA-MPC-DHVs@VEGF: The MADHVs were developed with the precursor solution (15% PEGDA, 15% MPC, and initiator 0.06% LAP, w/v, 1 μ g/mL VEGF) as described above.

All the obtained heart valves were stored in sterilized and antibiotic-containing PBS at 4 °C for further experiments.

2.5. Characterization of hydrogel-coated hybrid heart valves

ATR-FTIR spectroscopy (INVENIO, Bruker, Germany) was used to verify the chemical compositions of all the sample surfaces. Scanning electron microscopy (SEM) was used to observe the microstructure of the heart valves. In a brief, samples were dehydrated by increasing gradient ethanol solutions (30%, 50%, 70%, 90%, 100%) for 15 min at each concentration and followed by CO₂ critical point drying. Then, the morphologies of the dried samples were observed by SEM (Nova NanoSEM 450, USA).

Immunohistochemical staining and VEGF quantification by ELISA were used to verify the efficient loading of VEGF in the PEGDA-MPC-DHVs@VEGF. Briefly, for immunostaining, sections were incubated with the primary antibody rabbit anti-human VEGF (1:100, Servicebio, Wuhan, China) and then visualized using a horseradish peroxidase (HRP)-labeled goat antirabbit IgG (1:200, Servicebio) and diaminobenzidine (DAB) kit (Servicebio). Cell nuclei were stained with hematoxylin. The images were captured by an automatic digital slide scanner (Pannoramic MIDI, 3DHISTECH Ltd. Budapest, Hungary). For VEGF quantification detected by ELISA in the samples, nearly 20 mg of sample tissue was homogenized at 4 °C to obtain supernatant, and the VEGF concentration was detected with the Human VEGF ELISA kit (Mukti Science, EK183-02) according to the manual and the absorbances at 450 nm were read with a microplate absorbance reader (BioTek,

Epoch).

The release property of loaded VEGF was assessed by ELISA to evaluate the release kinetics of VEGF in hydrogel. In a brief, 1000 ng/mL VEGF were added into the PEGDA-MPC hydrogel precursor and the photopolymerized to prepare PEGDA-MPC@VEGF hydrogel. Then the hydrogel was immersed in sterilized PBS in 37 °C incubator. The supernatants from the incubation solutions were withdrawn and frozen at -20 °C at the determined time points (1, 3, 5, 7, and 14 days). The quantitative measurement of the VEGF in the supernatants was performed using the Human VEGF ELISA Kit (Mukti Science, EK183-02) according to the manufacturer's specifications and the absorbances at 450 nm were read with a microplate absorbance reader (BioTek, Epoch).

2.6. Collagenase degradation

Collagenase degradation was performed to evaluate the stability of collagen in the heart valve. The heart valves (n = 6) were cut into 1 cm \times 1 cm pieces. Then, they were lyophilized and weighed. The weight obtained before collagenase degradation was recorded as W₀. Next, the heart valves were immersed in collagenase I solution (80 U/mL, dissolved in PBS) at 37 °C for 24 h and 48 h, respectively. Then, the samples were washed with deionized water and lyophilized again, and the obtained dry weight was recorded as W₁. The weight persistence after degradation (%) was calculated with the following formula:

$$\text{Weight persistence after degradation (\%)} = \frac{W_1}{W_0} \times 100\%$$

2.7. Uniaxial tensile test

The uniaxial tensile test was conducted via an electronic universal testing machine (BioTester, CellScale, Waterloo, Canada) to evaluate the characteristics of the heart valves. Briefly, samples of the different treatment groups (n = 5) were cut into 20 mm \times 5 mm strips along the collagen fiber direction and washed with PBS three times. Then, three random points on the surface of the heart valve were measured with a thickness tester, followed by averaging for further statistics. Each sample was pull tested at an extension rate of 12.5 mm/min until it fractured. The elastic modulus and stress-strain curve were obtained from the original data.

2.8. Adhesion assay of platelets in vitro

The platelet adhesion assay was performed to evaluate the thrombogenic properties of the heart valves. Platelet-rich plasma (PRP) was obtained by centrifugation from rabbit citrated whole blood (1:9 volume ratio of 3% sodium citrate to whole blood) at 1500 rpm for 15 min. The heart valves were cut into 1 cm \times 1 cm pieces and placed into 48-well plates. Then 500 μ L of PRP was added to the plates and incubated with the samples for 2 h at 37 °C. Then, the heart valves were fixed with 2.5% glutaraldehyde solution at 4 °C overnight. The heart valves were dried by CO₂ critical point drying and then the images were taken by SEM (Nova NanoSEM 450, USA). For the LDH assay, the samples were treated with 0.5% Triton X-100 (v/v) for 30 min at room temperature. The LDH activity in the lysed platelet suspension was detected by an LDH assay kit according to the manuals.

2.9. Ex vivo antithrombogenicity assay

Animal experiments were approved by the Ethical Committee of Sichuan University. The ex vivo antithrombogenicity assays were performed according to previous reports [29]. Samples of each treatment group (n = 6) were cut into 0.5 cm \times 1 cm strips and immersed in 75% ethanol overnight, followed by rinsing with normal saline three times. Then, the samples were constructed to tubes with an inner diameter of

about 3 mm and placed in the heparin-pres soaked silicone tubes (the inner diameter of silicone tube: 4.5 mm) (100 U/ml heparin solution). New Zealand white rabbits were anesthetized with isoflurane continuously. Then one side of the common carotid artery and the contralateral external jugular vein were carefully isolated and cannulated with a drainage tube. After 2 h of perfusion, the samples were removed and rinsed with normal saline to remove uncoagulated blood. Then, the samples were fixed with 2.5% glutaraldehyde solution and dehydrated with CO₂ critical point drying. A scanning electron microscope (Nova NanoSEM 450, USA) was used to observe the morphology of the samples.

2.10. Hemolysis rate assay

The citrated rabbit blood was centrifuged and diluted with normal saline to obtain a 2% erythrocyte suspension. The samples (1 cm × 1 cm) were placed into 24-well plates and incubated with 500 μL 2% erythrocyte suspension for 1 h at 37 °C with continuous shaking. Then, the supernatant was obtained by centrifugation at 1500 rpm for 15 min. The supernatant absorbance at 540 nm was detected by a microplate reader (Multiskan MK3, Thermo Fisher, USA). The treatment groups of erythrocyte suspensions treated with normal saline and deionized water were utilized as negative and positive controls, respectively. The hemolysis rate was calculated using the following equation:

$$\text{Hemolysis rate (\%)} = \frac{OD_{\text{sample}} - OD_{\text{negative}}}{OD_{\text{positive}} - OD_{\text{negative}}} \times 100\%$$

2.11. In vitro biocompatibility

2.11.1. In vitro cytotoxicity

To prepare the PEGDA-DHVs, PEGDA-MPC-DHVs, and PEGDA-MPC-DHVs@VEGF, MADHVs were dialyzed in deionized water at room temperature for 24 h and then sterilized in 75% ethanol for 24 h, followed by washing with sterilized PBS for at least for 5 times. The hydrogel precursors were filtered through a 0.22 μm filter before they were used to develop hydrogel-coated hybrid heart valves. The Glu-DHVs were sterilized in 75% ethanol for 24 h. The sterilized Glu-DHVs and hydrogel-coated hybrid heart valves were washed with sterilized PBS again at least five times. Extracts were prepared by immersing the heart valves into DMEM at a concentration of 0.1 g/mL for 24 h at 37 °C in a cell incubator. The human umbilical endothelial cells (HUVECs) were seeded in 96-well plates at a density of 2000 cells/well. After 8 h of incubation, the medium was replaced with 200 μL of the obtained extract medium for each well. Cells were cultured for 1, 3, and 5 days, and the culture extracts were replaced every two days. After culture, 100 μL of new medium and 10 μL of CCK-8 working solution were added to replace the previous medium and incubated for another 2 h. The absorbance of supernatant at 450 nm was read by a microplate reader (Multiskan MK3, Thermo Fisher, USA) to detect cell viability.

2.11.2. HUVEC proliferation

The sterilized heart valves were obtained as mentioned above. After being cut into 1 cm × 1 cm pieces and rinsed with sterilized with PBS, the samples were placed into 48-well plates. Then, HUVECs were seeded on the valves at a density of 4 × 10⁴ cells/mL and cultured for 1, 3, and 5 days. After incubation, the heart valves were transferred to a new 48-well plate, and 200 μL of DMEM and 20 μL of CCK-8 working solution were added to the culture for 2 h at 37 °C. The absorbance at 450 nm was read by a microplate reader to detect cell viability. For fluorescence microscopy, samples were stained with DAPI and TRITC-phalloidin. Cell morphology on the valves was immediately captured with a laser scanning confocal microscope (Olympus spin, Japan). After coculture with HUVECs, samples were fixed with 4% paraformaldehyde and HE staining and immunohistochemical (IHC) staining were conducted to evaluate the adhesion of HUVECs onto the heart valves. Rabbit antihuman Von Willebrand Factor was used to label endothelial cells adhered to the surface

of the heart valves. Images were obtained with an automatic digital slide scanner (Pannoramic MIDI, 3DHISTECH Ltd. Budapest, Hungary).

2.12. Subcutaneous implantation

Animal experiments were approved by the Ethical Committee of Sichuan University. The heart valves were cut into 1 cm × 1 cm pieces and sterilized as mentioned above. Each treatment group of heart valves was implanted subcutaneously and randomly in each SD rat. In brief, the 180–200 g male SD rats were anesthetized with pentobarbital sodium and four dorsal surgical incisions were made on the back of each rat and the samples were implanted subcutaneously. 30 days after the implantation, samples with fibrous capsules were resected. The excised tissue was utilized for histology and calcium content analysis.

2.12.1. Calcium deposition assay

Briefly, the fibrous tissue attached to the heart valve was carefully removed by tweezers. Then the obtained heart valves were freeze-dried, weighed and dissolved in 6 M HCl for 24 h at 60 °C. The supernatants were collected, filtered and diluted 40-fold in deionized water before ICP-OES (5100 SVDV, Agilent, USA) analysis.

2.12.2. Histological and immunohistochemical assay

The freshly fixed valves of the group Glu-DHVs, PEGDA-DHVs, PEGDA-MPC-DHVs, and PEGDA-MPC-DHVs@VEGF treatment groups were stained with HE, Masson, alizarin and immunohistochemical staining. H&E staining and alizarin red staining were utilized to visualize the cells and verify the calcium deposition, respectively. Masson staining were utilized to verify collagen fibers. As for immunohistochemical (IHC) staining, rabbit anti-rat F4/80 antibody and rabbit anti-rat CD3 antibody were utilized to label macrophages and T cells, respectively. Cell nuclei were stained with hematoxylin.

2.13. Statistical analysis

All experimental results are presented as the mean ± standard deviation (SD). One-way analysis of variance was performed for statistical analyses of the data. A P value < 0.05 was considered statistically significant.

3. Results

3.1. Optimization of hybrid hydrogel composition and VEGF concentration

Zwitterionic hydrogels with various amounts of MPC were prepared to optimize the anti-biofouling property. As shown in Fig. S1a, the water contact angle of the PEGDA hydrogel was 35.75 ± 6.60°. The water contact angle of hydrogels decreases as more MPC was added to the hydrogels, which indicated that adding MPC increases the hydrophilic properties of hydrogels. As shown in Fig. S1b, the protein adsorption content on the surface of the PEGDA hydrogels were approximately 14.98 ± 0.70 μg/cm². With the addition of MPC to the hydrogel, the adsorption content on the surface decreased. As shown in Fig. S2a, less cell adhesion was observed on the pure hydrogel substrate compared to the TCP control (the blank orifice plates without hydrogel treatment), which indicated a better anti-biofouling property of the hydrogel. Moreover, with the addition of more MPC to the hydrogels, the zwitterionic hydrogels showed better anti-cell adhesion properties than the PEGDA hydrogels. The quantitative results of the adhered cells are shown in Fig. S2b. PEGDA-15%MPC was chosen as the optimized composition of the hybrid hydrogels for further experiments.

VEGF was used to facilitate the proliferation and adhesion of endothelial cells. As shown in Fig. S3a, the PEGDA-MPC hydrogels exhibited the least cell adhesion on the surface. With the addition of VEGF to the hydrogels, more cell adhesion was observed on the surface of the hydrogel compared to the PEGDA-MPC hybrid hydrogels. The

quantitative results of adhesion cells in Fig. S3b showed a significant difference between the PEGDA-MPC treatment group and the PEGDA-MPC-DHVs+1.0 $\mu\text{g}/\text{mL}$ VEGF treatment group, while no significant difference was observed between the PEGDA-MPC treatment group and the PEGDA-MPC-DHVs+0.5 $\mu\text{g}/\text{mL}$ VEGF treatment group, which indicated that a higher concentration of VEGF leads to better proliferation and adhesion of endothelial cells. In addition, with increasing concentrations of MPC, the hybrid hydrogels did not exhibit much cytotoxicity, as shown in Fig. S4. As a result, PEGDA-MPC-DHVs+1.0 $\mu\text{g}/\text{mL}$ VEGF was chosen for further experiments.

3.2. Characterization of DHVs, MADHVs, and PEGDA-MPC-DHVs@VEGF

Masson staining and H&E staining were used to confirm the efficiency of decellularization of the heart valves. As shown in Fig. S5, no cells were found in the DHV samples. MA was grafted onto DHVs via a reaction between amino groups and anhydride. ^1H NMR was utilized to directly verify the successful grafting of MA into the DHVs. As shown in Fig. 2a two obvious peaks (5.3 ppm and 5.6 ppm) were observed in the MADHVs compared with the DHVs, which indicated the successful grafting of the vinyl groups on MADHVs.

The content of remnant amino groups can indirectly reflect the grafting degree of MA. As shown in Fig. 2c, the lower content of remnant

amino groups indicated a higher grafting degree of vinyl groups in the MADHVs. With the increase in feed ratio from 0.1 to 1.0, the amino content significantly decreased. However, the content of remnant amino groups did not decrease significantly despite the feed ratio increasing from 1.0 to 3.0, which indicated that the reaction between amino groups and MA reached a saturated state. The feed ratio of 1.0 was chosen for further experiments.

FTIR was used to characterize the composition and successful grafting of PEGDA and MPC onto the surface of the MADHVs. As shown in Fig. 2b, the FTIR spectra of the PEGDA and PEGDA-DHVs showed the same peaks at 840 cm^{-1} , $1237\text{--}1280\text{ cm}^{-1}$, 1775 cm^{-1} , and 2876 cm^{-1} , which represented the rocking vibration CH_2 of $\text{CH}_2\text{CH}_2\text{O}$, asymmetric stretching $\text{C}=\text{O}$ of COOC , and symmetric stretching CH_2 respectively. The same peak between the PEGDA and PEGDA-DHVs indicated that the DHV samples were fully covered by PEGDA hydrogels. In addition, compared to the FTIR peak of the PEGDA hydrogel, the spectrum of the PEGDA-MPC-DHV sample indicated additional peaks at 960 cm^{-1} , which indicated the occurrence of $-\text{N}^+(\text{CH}_3)_3$, at 1080 cm^{-1} and 1237 cm^{-1} , which were ascribed to $\text{P}=\text{O}$ stretching and $\text{P}-\text{O}$ stretching, respectively. The FTIR results demonstrate the successful grafting of MPC molecules into the PEGDA hydrogel. And the results in Fig. S6 show that the dry weight remaining of hydrogel is decreasing with the time increasing, which indicates that the PEGDA, PEGDA-MPC, and PEGDA-MPC@VEGF hydrogels are degradable.

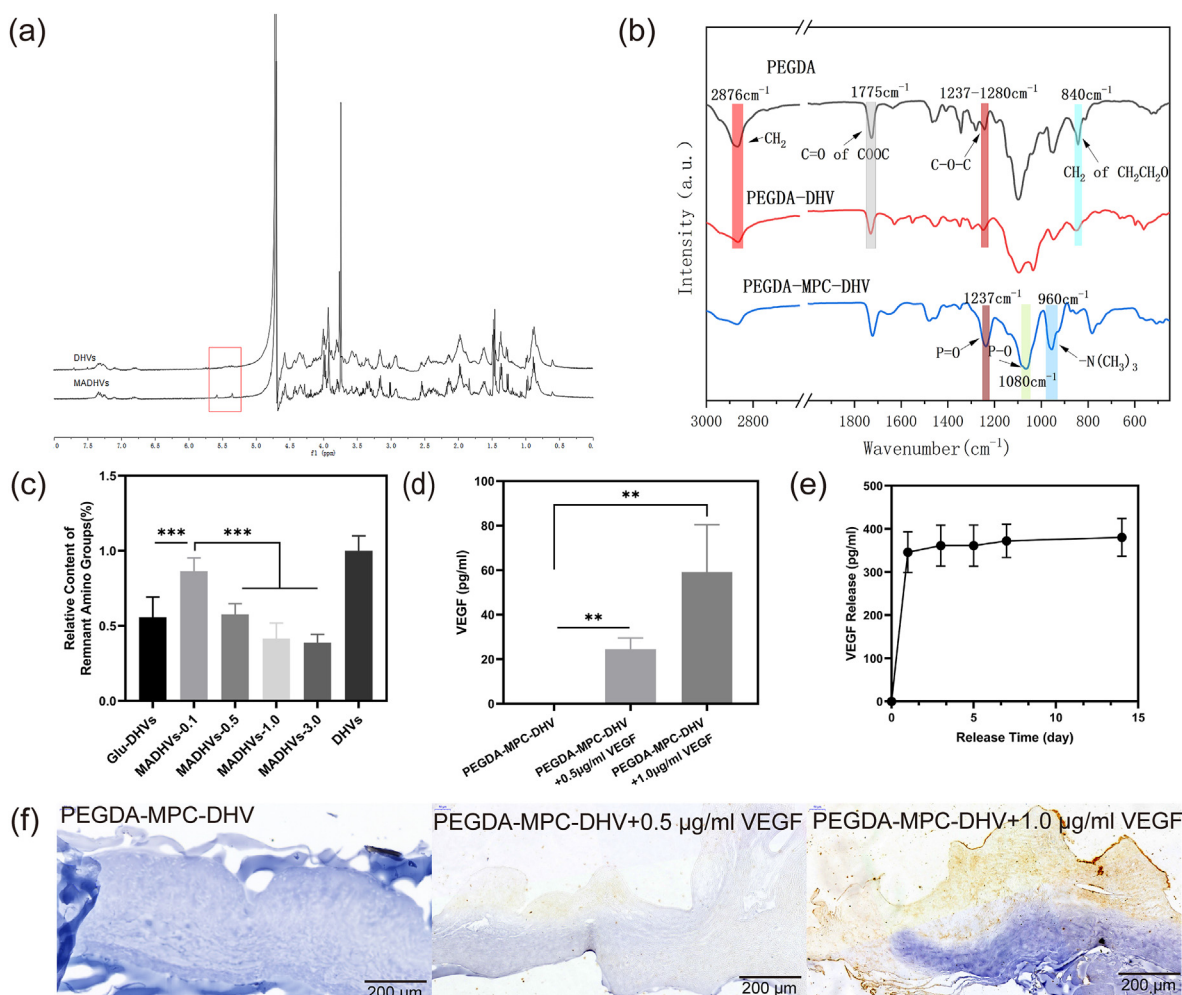


Fig. 2. Characterization of the hybrid hydrogel heart valve. (a) ^1H NMR spectra of MADHVs and DHVs. (b) FTIR spectra of PEGDA hydrogel, PEGDA-DHVs and PEGDA-MPC-DHVs. (c) Relative content of remnant amino groups detected by the ninhydrin assay ($n = 6$). (d) VEGF in hydrogel-hybrid heart valve quantified by ELLISA ($n = 5$). (e) The in vitro cumulative release of VEGF in hydrogel over a span of 14 days ($n = 3$). (f) Representative VEGF immunostaining (*anti*-VEGF) images for the hybrid hydrogel heart valves of PEGDA-MPC-DHV+0.5 $\mu\text{g}/\text{mL}$ VEGF and PEGDA-MPC-DHV+1.0 $\mu\text{g}/\text{mL}$ VEGF groups.

VEGF quantification and immunohistochemical staining were utilized to characterize the efficient loading of VEGF in the hybrid hydrogel heart valves. Fig. 2d shows that the amount of total loaded VEGF in the PEGDA-MPC-DHV@VEGF increased with increasing VEGF content. Compared with the PEGDA-MPC-DHVs, more brown VEGF staining was observed in the PEGDA-MPC-DHVs+1 $\mu\text{g}/\text{mL}$ VEGF by immunostaining (Fig. 2f). These results confirmed that VEGF was successfully and efficiently loaded in the hybrid hydrogel heart valve system.

The in vitro release kinetics of VEGF was quantified in PBS at 37 °C for up to 14 days. As shown in Fig. 2e, an initial important and rapid release of VEGF from the PEGDA-MPC@VEGF hydrogel was observed within 24 h. The total amount of VEGF released during 14 days reached about 380.45 ± 43.78 $\mu\text{g}/\text{mL}$.

3.3. Morphologies of heart valves

As shown in SEM in Fig. 3, the surface of the Glu-DHVs seemed rough and obvious collagen fibers lined the surface. However, the surface of the heart valve modified by the hydrogel appears smooth, and the cross-section images show a clear boundary lines between the heart valves and hybrid hydrogel films.

3.4. Collagen stability

Collagenase degeneration in vitro was used to evaluate the stability of collagen. As shown in Fig. 4a, the weight persistence ratios of the Glu-DHVs, PEGDA-DHVs, PEGDA-MPC-DHVs, and PEGDA-MPC-DHVs@VEGF were $35.04 \pm 9.63\%$, $94.71 \pm 2.62\%$, $92.63 \pm 1.67\%$, $90.02 \pm 2.48\%$, and $90.04 \pm 4.68\%$ after 24 h of collagen I treatment and $38.66 \pm 9.35\%$, $94.86 \pm 4.06\%$, $85.11 \pm 11.22\%$, $89.94 \pm 5.03\%$, and $85.19 \pm 3.36\%$ after 48 h of collagen I treatment, respectively, which were much higher than that of the DHVs. Moreover, no significant difference in the weight persistence ratio was observed among the Glu-DHVs, PEGDA-DHVs, PEGDA-MPC-DHVs, and PEGDA-MPC-DHVs@VEGF, which indicated that similar collagen stability can be achieved by free radical polymerization compared to the Glu-DHVs. This result indicates that hybrid coating treatment can provide comparative collagen stability after implantation.

3.5. Mechanical property

As shown in Fig. 4b, the elastic moduli of the Glu-DHVs (10.08 ± 1.33 MPa) were significantly higher than that of the PHVs (6.79 ± 2.12 MPa), DHVs (5.95 ± 1.71 MPa), PEGDA-DHVs (6.50 ± 0.60 MPa), PEGDA-MPC-DHVs (6.24 ± 1.05 MPa) and PEGDA-MPC-DHVs@VEGF (6.38 ± 1.02 MPa). However, no significant difference was observed among the elastic moduli of the PHVs, DHVs, PEGDA-DHVs, PEGDA-MPC-DHVs,

and PEGDA-MPC-DHVs@VEGF. Moreover, no significant difference in fracture strain was observed among the six groups as shown in Fig. 4c. The stress-strain curves are shown in Fig. S7.

3.6. Hemocompatibility

Platelet adhesion and hemolysis rate assays were performed to evaluate the hemocompatibility performance of the heart valves. As shown in Fig. 5a, various platelets were observed to adhere to the surface of the Glu-DHVs and PEGDA-DHVs, while less platelet adhesion was seen on the surface of the PEGDA-MPC-DHV and PEGDA-MPC-DHVs@VEGF, which indicated that the zwitterionic monomer MPC improved anti-platelet adhesion on the surface of heart valves. Moreover, LDH quantification in Fig. 5b showed that the LDH activity of the PEGDA-MPC-DHVs and PEGDA-MPC-DHVs@VEGF was significantly lower than that of the Glu-DHVs, which indicated significantly less platelet adhesion in the PEGDA-MPC-DHVs and PEGDA-MPC-DHVs@VEGF than in the Glu-DHVs.

The hemolysis rates of Glu-DHVs, PEGDA-DHVs, PEGDA-MPC-DHVs, and PEGDA-MPC-DHVs@VEGF in Fig. 5c were $1.20 \pm 0.32\%$, $0.91 \pm 0.38\%$, $0.60 \pm 0.21\%$, and $1.13 \pm 0.29\%$, respectively and the hemolysis rates of the four treatment groups were all lower than 5%. There was no significant difference in hemolysis among the four groups. The hemolysis assay images are shown in Fig. S8.

The ex vivo antithrombogenicity assay was further used to evaluate the integrated hemocompatibility of the heart valves within a physiological status as shown in Fig. 6a. After exposure of the heart valves to blood in ex vivo blood circulation for 2 h, a large amount of thrombus formed on the surface of the Glu-DHVs and PEGDA-DHVs whereas there was little blood clotting on the surface of the PEGDA-MPC-DHVs and PEGDA-MPC-DHVs@VEGF samples (Fig. 6b and c). Moreover, the SEM results in Fig. 6d show that in the Glu-DHVs samples, there was a massive number of activated platelets and erythrocytes trapped in the fibrin network. In contrast, there were few adhered platelets and erythrocytes, which was consistent with the macroscopic phenomenon. Therefore, the PEGDA-MPC-DHVs and PEGDA-MPC-DHVs@VEGF samples exhibit better hemocompatibility than the Glu-DHVs.

3.7. In vitro cytotoxicity

A cytotoxicity assay of the heart valve extracts was performed to evaluate the cytotoxicity of the heart valves. As shown in Fig. 7a, there was no significant difference in cell viability among the four treatment groups, and the cell viability of all four groups was higher than 80%, which indicated that the heart valve coated with hydrogel exhibited no cytotoxicity.

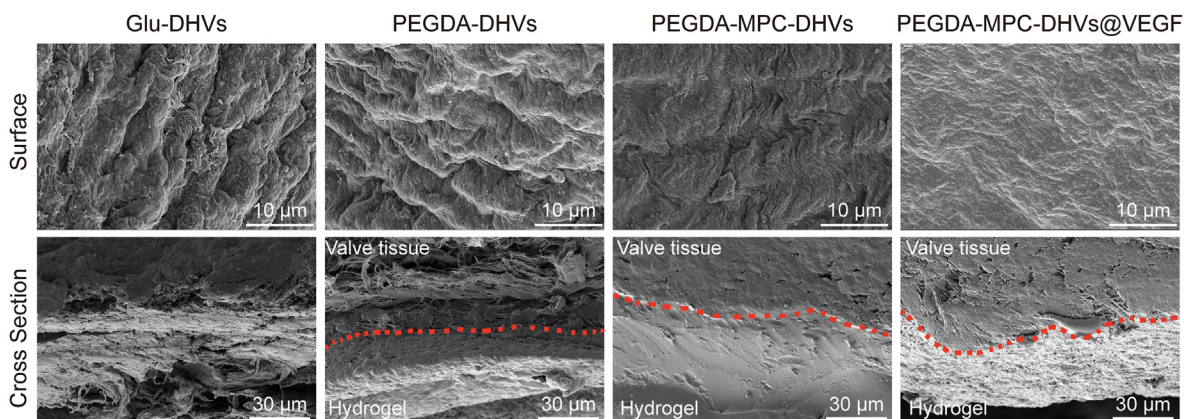


Fig. 3. Morphologic characterization of the heart valves. (a) Surface and (b) cross section images of the heart valves observed by SEM in the Glu-DHVs, PEGDA-DHVs, PEGDA-MPC-DHVs, and PEGDA-MPC-DHVs@VEGF groups.

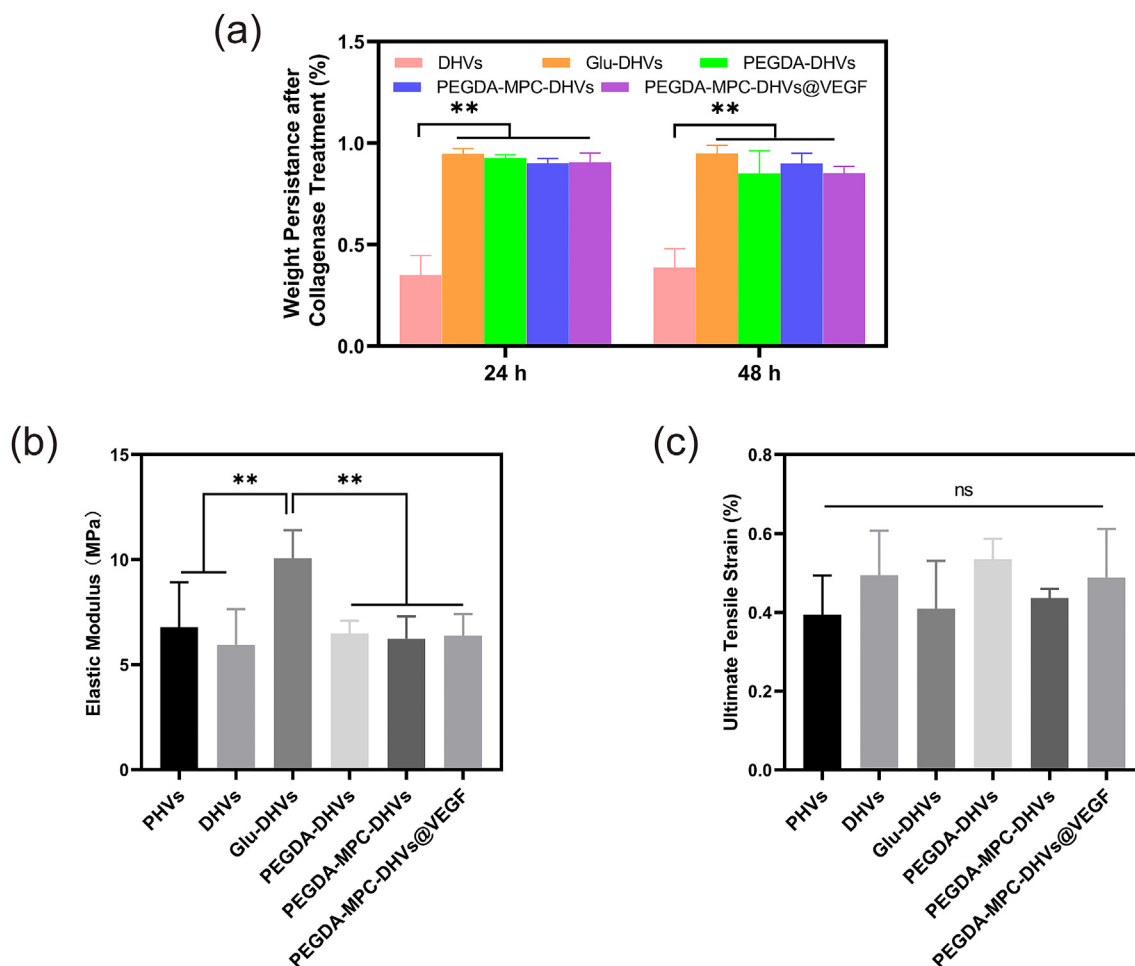


Fig. 4. Collagen stability and mechanical properties of the heart valves. (a) Weight persistence ratio after collagenase I treatment for 24 h and 48 h ($n = 6$). (b) Elastic modulus ($n = 5$) and (c) fracture strain of the heart valves in groups PHVs, Glu-DHVs, PEGDA-DHVs, PEGDA-MPC-DHVs and PEGDA-MPC-DHVs@VEGF ($n = 5$), respectively. * indicates $P < 0.05$ and ** indicates $P < 0.01$.

3.8. HUVEC proliferation on the heart valves

HUVEC proliferation on the heart valve surface reflected the endothelialization potential of the hydrogel-coated heart valves. According to the CCK-8 results shown in Fig. 7b, the cell viability of the PEGDA-DHVs and PEGDA-MPC-DHVs@VEGF was much higher than that of Glu-DHVs on the 3rd and 5th days, which indicated that more endothelial cells were seeded on the surface of the PEGDA-DHVs and PEGDA-MPC-DHVs@VEGF. Moreover, the cell viability of PEGDA-MPC-DHVs was lower than that of PEGDA-MPC-DHVs@VEGF, which indicated that VEGF promoted endothelial cell adhesion and proliferation on the surface of heart valves. As shown in Fig. 7c, the PEGDA-MPC-DHVs@VEGF exhibited the most endothelial cells on the 3rd and 5th days, while nearly no cell adhesion or proliferation was observed on the surface of the Glu-DHVs, which was consistent with the CCK-8 results. Moreover, the HE and VWF immunohistochemistry in Fig. S9 shows that more endothelial cells adhered to the surface of the PEGDA-MPC-DHVs@VEGF than that of the Glu-DHV after coculture with HUVECs for 5 days.

3.9. Biocompatibility

After 30 days of subcutaneous implantation in the rats, the heart valve samples were subjected to histological and immunohistochemical staining, which was utilized to evaluate the biocompatibility and immune response of the heart valves. As shown in Fig. 8a, HE staining images showed that there were large amounts of inflammatory cells on the

interface between the implanted heart valves and the surrounding fibrous capsule, and some inflammatory cells could even be seen infiltrating deep into the heart valve tissue in the Glu-DHV group. However, fewer cells were recruited around the implanted heart valve in the other groups. And the Masson staining images in Fig. 8b showed the collagen structure of heart valve and the hydrogel on the surface and among the collagens can be observed in the hydrogel-hybrid heart valves.

Then, to further evaluate the immune response, biomarkers such as F4/80 and CD3 were utilized to verify the phenotype of the inflammatory cells around the implanted heart valves. In immunohistochemical staining, the inflammatory cells marked by F4/80 and CD3 antibodies were macrophages and T cells, respectively. As shown in Fig. 9, for all samples, various F4/80-marked macrophages were distributed around the interface between the samples and surrounding tissue, while fewer CD3-marked T cells were observed around the samples. In the immune response, macrophages seemed more active than the T cells, especially the Glu-DHVs. More macrophages and T cells were distributed around the sample tissues in the Glu-DHV groups than in the hydrogel-hybrid heart valve groups, which indicated that the hydrogel coating elicited a much-mitigated immune response than the Glu-DHVs. Moreover, there were more recruited macrophages than CD3-positive T cells in the four groups.

3.10. In vivo calcification

Alizarin red staining and calcium quantitation by ICP-OES were utilized to determine the calcification degree of heart valves after 30 days of

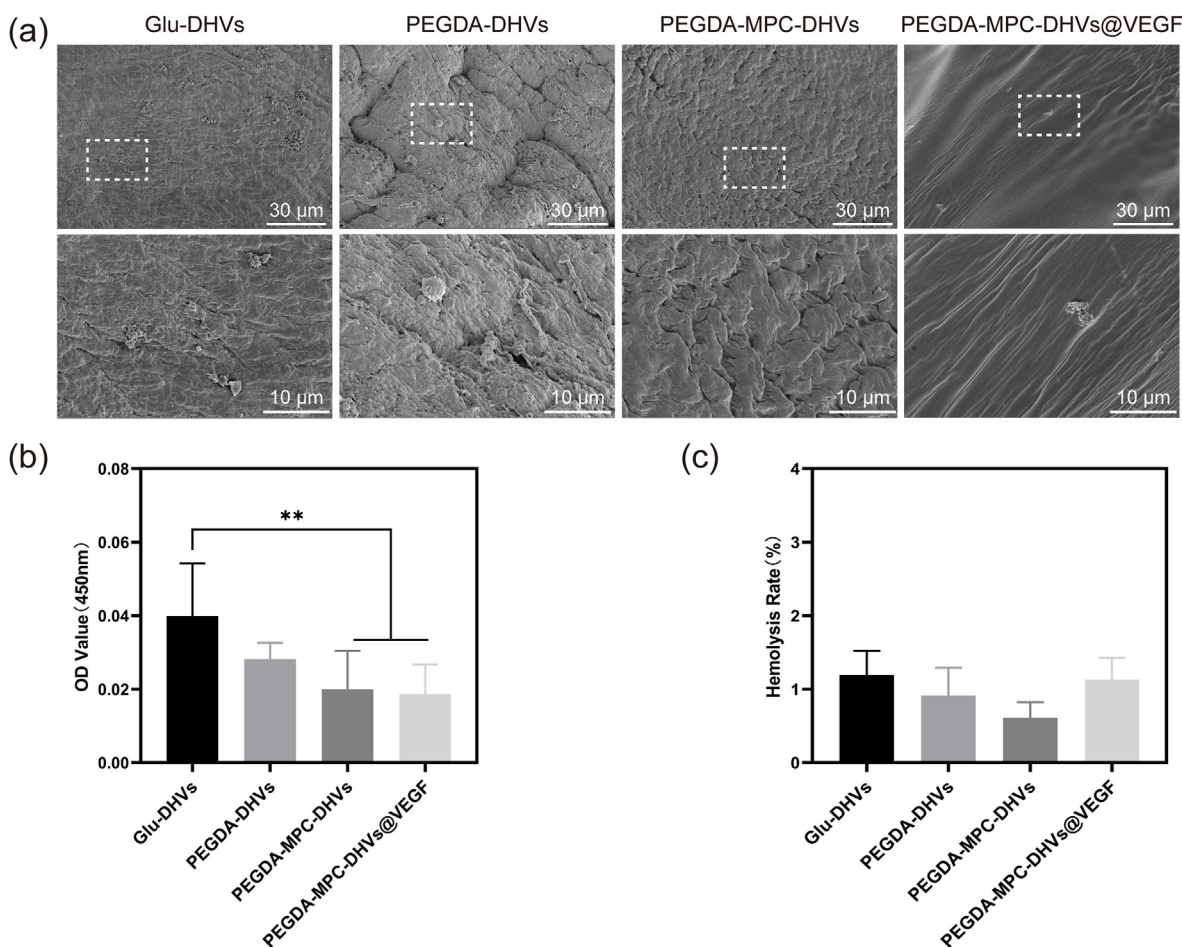


Fig. 5. Hemocompatibility of the heart valves. (a) SEM images of the heart valves after incubation with platelet-rich plasma. (b) LDH quantification of adhered platelets on the heart valves (n = 6). (c) Hemolysis rate of the heart valves in groups Glu-DHVs, PEGDA-DHVs, PEGDA-MPC-DHVs, and PEGDA-MPC-DHVs@VEGF (n = 5), respectively. ** indicates P < 0.01.

implantation. As shown in Fig. 10a, a high degree of calcium deposition, dyed orange, can be observed in the heart valve tissue in the Glu-DHVs, which indicated that heart valve calcification occurred. However, less calcium deposition was observed in the other treatment groups. ICP-OES, which determined the calcification quantitation of the heart valves, is shown in Fig. 10b. The calcium contents of the Glu-DHVs, PEGDA-DHVs, PEGDA-MPC-DHVs, and PEGDA-MPC-DHVs@VEGF were 1.66 ± 0.67 μg/mg, 0.86 ± 0.10 μg/mg, 1.03 ± 0.07 μg/mg, and 0.85 ± 0.25 μg/mg, respectively. Significant differences were observed among the Glu-DHV group and PEGDA-DHVs, PEGDA-MPC-DHVs, and PEGDA-MPC-DHVs@VEGF groups. However, there was no significant difference among the PEGDA-DHVs, PEGDA-MPC-DHVs, and PEGDA-MPC-DHVs@VEGF groups. The results suggested that the zwitterionic hydrogel-coated heart valves exhibited higher anti-calcification properties compared with the Glu-DHVs.

4. Discussion

Currently, bioprosthetic heart valves are popular in the clinic due to their excellent natural structure and hemodynamic characteristics. However, clinically used bioprosthetic heart valves, which are cross-linked with glutaraldehyde, still exhibit some drawbacks such as calcification, cytotoxicity, triggering an immune response, and thrombogenesis [16,30–33]. Cytotoxicity of glutaraldehyde can lead to failure of endothelialization of the heart valve, which is crucial to their lifespan. These drawbacks lead to the failure of glutaraldehyde-crosslinked heart valves between 12 and 15 years [31].

Therefore, anti-calcification, coagulation deactivation and endothelialization of prosthetic heart valves are considered important for prolonging their lifespan of heart valves.

Nonglutaraldehyde crosslinker and anti-biofouling material have been used to modify bioprosthetic heart valves to improve anti-calcification and biocompatibility [21,34]. For example, zwitterionic monomers, such as SBMA, have been used to coat heart valves and exhibit excellent antiadhesion of proteins, platelets and cells and improved anti-calcification and biocompatibility [22]. However, this repealing of the nonspecific adhesion of cells can lead to failure of endothelial cell adhesion, which is not beneficial for rapid re-endothelialization of heart valves and their long-term stability. Therefore, in this study, we developed a hydrogel hybrid-coated heart valve from porcine heart valves, zwitterionic monomers MPC, and VEGF to improve anti-biofouling, anti-calcification and biocompatibility. First, we used porcine heart valves as scaffolds for the bioprosthetic heart valves. Second, the heart valves are grafted by vinyl groups through reactions between amino groups and anhydrides, which were used to crosslink collagen and provide chemical bonds between the heart valves and hydrogels. Third, the zwitterionic hydrogel was coated onto the surface of the MADHVs via photoinitiated radical polymerization. Furthermore, to improve the endothelialization of the heart valve, VEGF was loaded into the zwitterionic hydrogel system. As a result, the hybrid hydrogel-coated heart valves could be developed with anti-calcification, anti-biofouling and rapid endothelialization properties.

Decellularization has been considered a way of deactivating the immune response and calcification [35–37]. To affirm the efficiency of

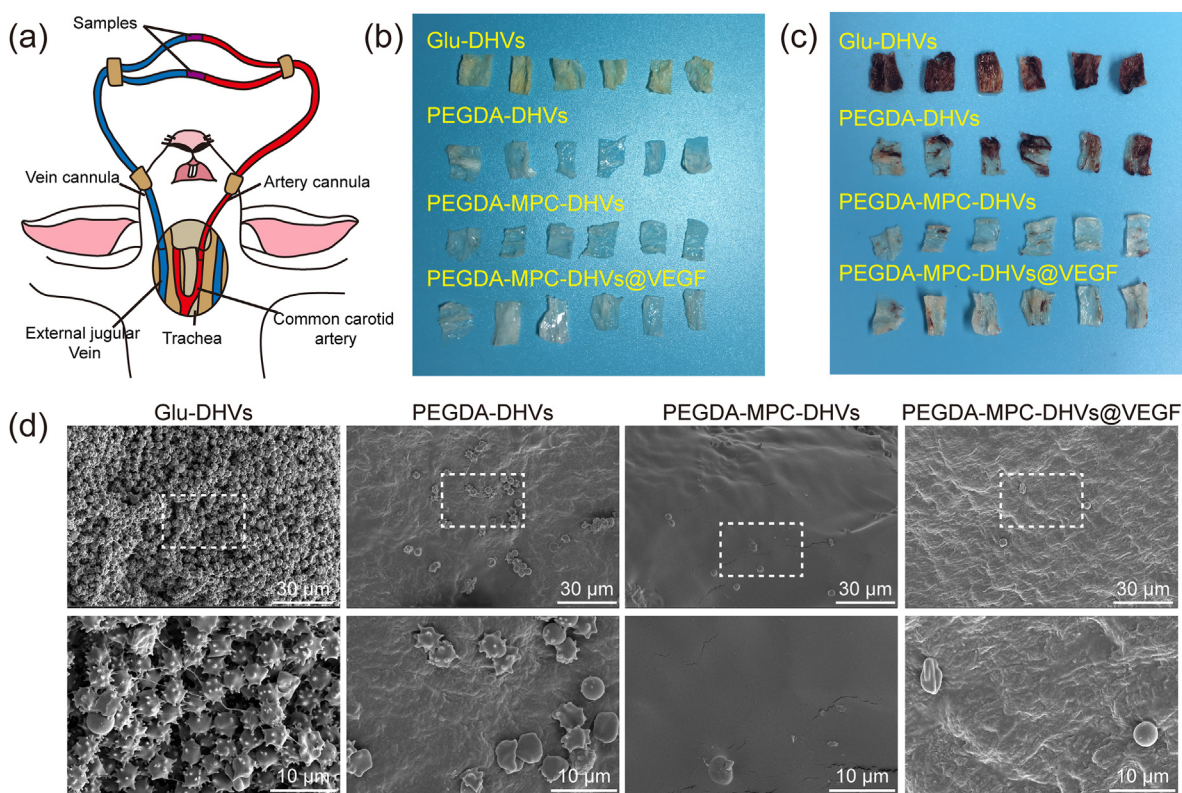


Fig. 6. Ex vivo antithrombogenicity assay. (a) Intraoperative image of the establishment of ex vivo blood circulation. (b) Photos of the heart valve samples before the test and (c) after the test. (d) SEM images of the heart valves in the Glu-DHVs, PEGDA-DHVs, PEGDA-MPC-DHVs and PEGDA-MPC-DHVs@VEGF groups after the ex vivo antithrombogenicity assay.

decellularization, HE and Masson staining were performed and the results of decellularization showed that no cells remained in the heart valves.

The surface of the natural porcine heart valves exhibits limited hemocompatibility and immune response. Therefore, PEGDA-MPC zwitterionic hydrogels were coated on the surface of native heart valves. To crosslink collagen and provide chemical bonds for the hydrogel precursor, vinyl groups were grafted onto the heart valves. ^1H NMR spectra also demonstrated successful grafting of vinyl groups into the DHVs and FTIR spectra demonstrated that PEGDA and MPC molecules were grafted in the PEGDA-MPC hydrogel-coated heart valve.

VEGF is a protein that can promote the adhesion and proliferation of endothelial cells and has been utilized to promote re-endothelialization of implanted cardiovascular devices [38–40]. In this study, VEGF was loaded in a hybrid hydrogel, which can function as a drug delivery system in medical fields. In the next experiments, we then demonstrated the efficiency of VEGF loading on the PEGDA/MPC hybrid hydrogel by VEGF staining. Our results showed that VEGF was effectively present on the surface of the heart valves. The in vitro release kinetics of VEGF demonstrate that the most VEGF was released within 1 day, when VEGF can play a role in promoting adhesion and proliferation of endothelial cells. However, the defect of hydrogel loaded with VEGF is the uncontrolled rapid releasing within the early time. Moreover, we performed HUVEC culture experiments and found enhanced HUVEC adhesion and proliferation on VEGF-loaded hybrid hydrogel heart valves via fluorescence microscopy and CCK-8 cell viability quantification. Thus, loaded VEGF can improve HUVEC adhesion and proliferation, which exhibits the improved re-endothelialization potential of heart valves.

Collagen, the main component of the heart valve, has been recognized as crucial for structural stability and mechanical properties. Glutaraldehyde has been reported to increase the stability of collagen because of its ability to increase the cross-linking of collagen fibers through Schiff base

reactions. It has been reported that the stability of collagen in methacrylated DHVs can also be improved via radical polymerization of vinyl [5]. Crosslinking via radical polymerization of the heart valve shows comparable collagen stability compared with glutaraldehyde treatment. In our study, the hybrid hydrogel-coated heart valves showed similar weight persistence after collagenase treatment, which indicates that they have comparable collagen stability compared with that of the Glu-DHV. Therefore, the improved collagen stability, compared to the control, is from crosslinking via radical polymerization. Moreover, we hypothesize that hydrogel film can act as a barrier to protect the collagenase bonding site in the heart valve from exposure to collagen, thus decreasing the degeneration of collagen. The results of the subcutaneous implantation assay showed that almost intact collagen structures can be maintained for hybrid hydrogel-coated heart valves.

The proper mechanical properties of the bioprosthetic heart valve play a crucial role in maintaining the normal function of opening and closing. According to previous studies, the elastic moduli of the natural aortic leaflet are 3–15 MPa in the circumferential direction and 1–2 MPa in the radial direction [41]. In our results, the hybrid hydrogel coating treatment did not significantly improve the elastic moduli compared with that of the DHVs, while the glutaraldehyde treatment significantly improved the mechanical properties compared with DHVs. It might be associated with degree of crosslinking in PEGDA-MPC-DHVs@VEGF, which is lower than that of Glu-DHVs [28]. However, the elastic moduli of hybrid hydrogel-coated heart valves remained within the range of elastic moduli of natural aortic valve leaflets, which indicated that PEGDA-MPC-DHVs@VEGF can exhibit comparable mechanical properties to natural heart valves. Moreover, excessive crosslinking of collagen might lead to high stiffness of heart valves and sacrifice the compliance, thus negatively affecting the opening and close function of heart valves [42].

Blood compatibility is considered essential for implanted

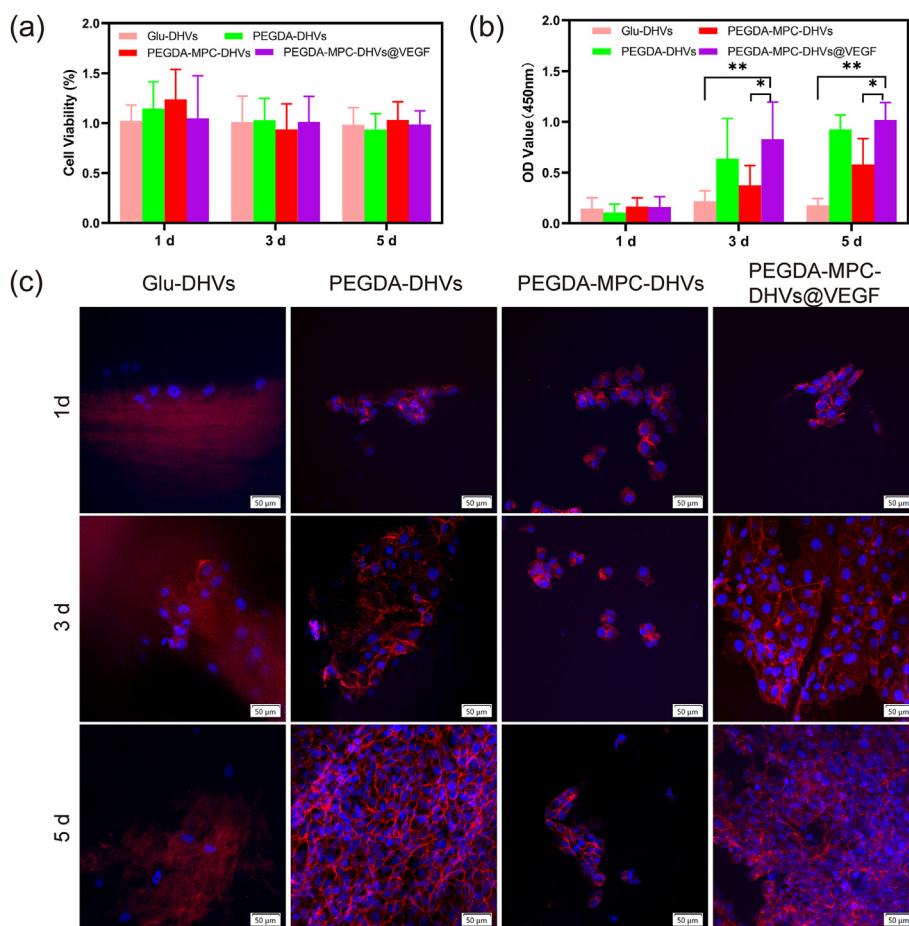


Fig. 7. In vitro biocompatibility of the heart valves. Cell viabilities of the HUVECs after culturing with (a) the extraction and (b) seeding on the surface of the heart valves of the Glu-DHVs, PEGDA-DHVs, PEGDA-MPC-DHVs and PEGDA-MPC-DHVs@VEGF groups for 1 day, 3 days, and 5 days, respectively (n = 6); (c) Fluorescence images of the HUVECs being seeded on the heart valves in the Glu-DHVs, PEGDA-DHVs, PEGDA-MPC-DHVs and PEGDA-MPC-DHVs@VEGF groups, respectively, for 1 day, 3 days, and 5 days. * indicates P < 0.05, ** indicates P < 0.01.

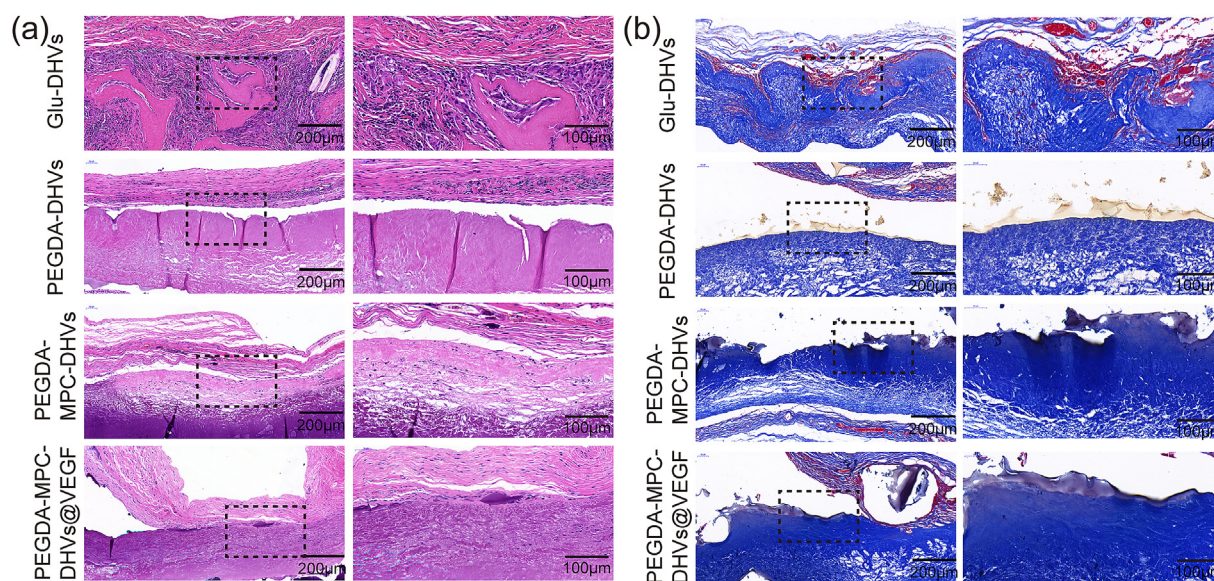


Fig. 8. (a) HE and (b) Masson staining images of heart valves after subcutaneous implantation for 30 days.

cardiovascular devices and undesirable protein absorption, and platelet adhesion leads to dysfunction and a decreased lifespan of implants. Thrombosis on artificial heart valves may result in stent occlusion or influence their opening and closing function, even leading to severe complications such as stroke [43]. Although glutaraldehyde-crosslinked heart valves show good hemocompatibility and hemodynamic

characteristics, thrombosis still occurs in patients who undergo bio-prosthetic heart valve surgery [3,44]. Protein adsorption and platelet adhesion are not inevitable on the surface of glutaraldehyde-crosslinked heart valves, which might lead to thrombosis. Previous studies showed that zwitterion polymer hydrogels exhibited excellent anti-biofouling (ability to repeal proteins and microbe adhesion onto the surface of

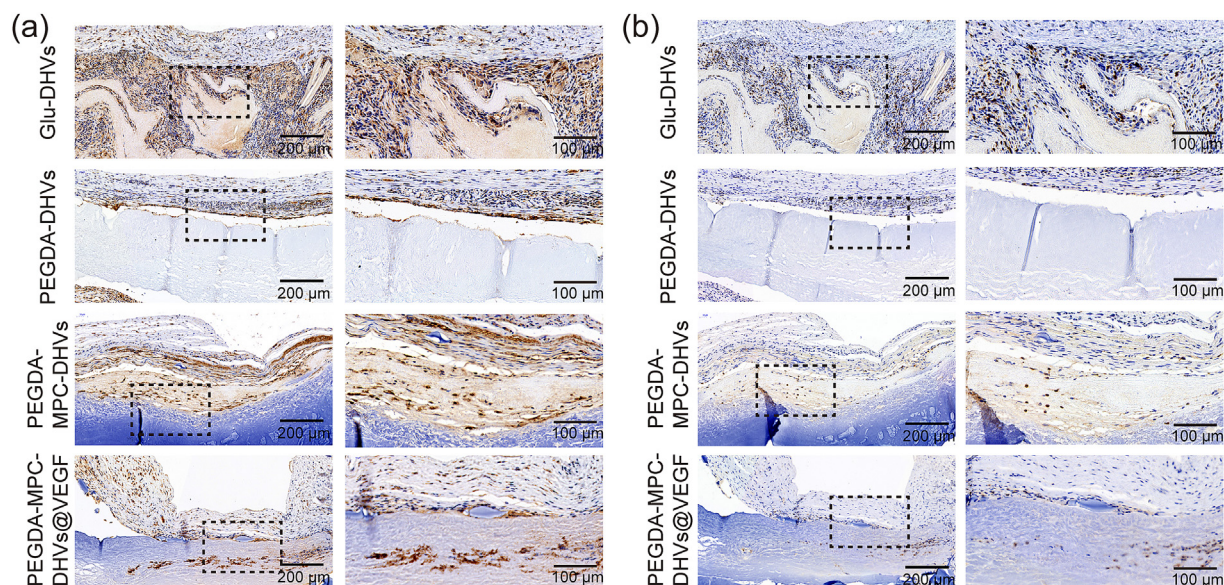


Fig. 9. Immune response elicited by the heart valves after subcutaneous implantation in rats for 30 days. Representative IHC images stained with (a) F4/80 and (b) CD3.

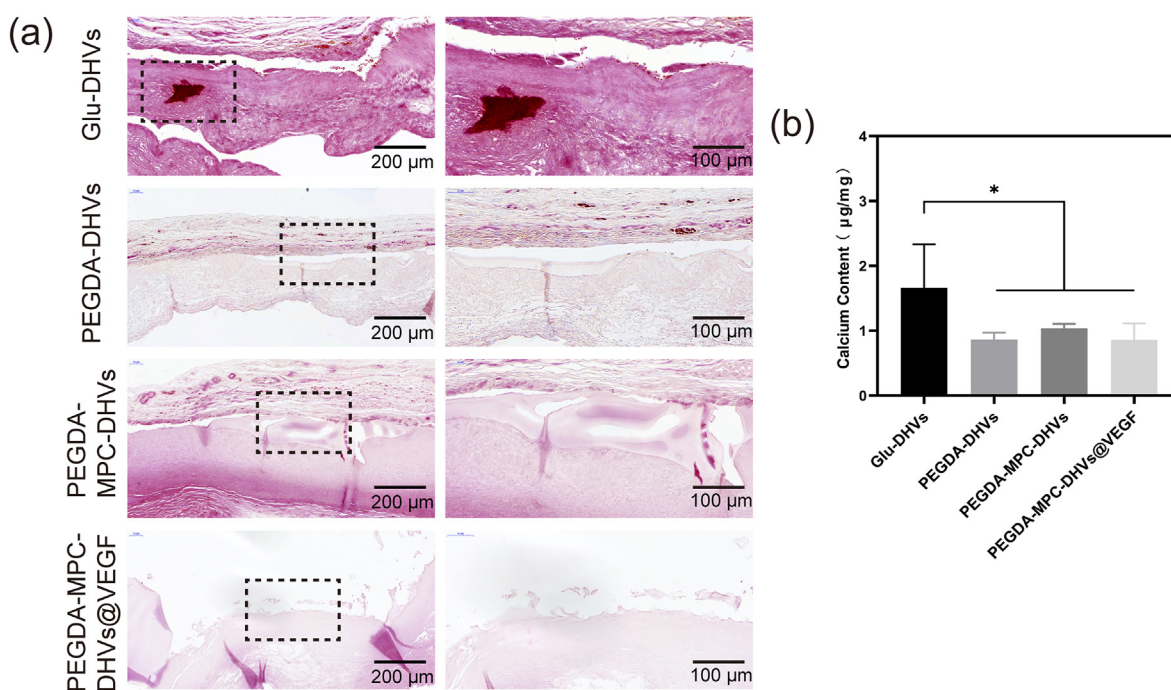


Fig. 10. In vivo calcification after subcutaneous implantation for 30 days. (a) Alizarin red staining images and (b) quantitative analysis of calcium content by ICP-OES (n = 5). * indicates P < 0.05.

materials) and biocompatibility properties [45,46]. PEGDA functions as a crosslinker and exhibits good hydrophilicity and biocompatibility and thus has been used in many fields of medicine, such as tissue engineering [47] and drug delivery systems [48]. Zwitterion polymers contain equal amounts of anionic and cationic groups, thus exhibiting electrical neutrality, and a stable hydrated layer can be formed by the ionic solvation of cationic and anionic groups, which leads to anti-biofouling properties [49–51]. And the hydration layer can avoid favorable interaction with protein molecules. As for the implants in cardiovascular systems, the activation of coagulation first originates from the biofouling. Plasma protein adhesion can lead to activation of complement, thus

further supporting platelet adhesion and activation. Then activated platelets initiate coagulation activation ending with the generation of thrombin and fibrin and thrombus formation [52]. Therefore, anti-biofouling property of implants modified with zwitterionic polymers can lead to improved hemocompatibility. Zwitterionic monomers such as SBMA and MPC have been used in cardiovascular devices due to their excellent hemocompatibility and antibiofouling properties [22,53]. In our study, zwitterionic monomer MPC was assembled in the PEGDA hydrogel, and this hybrid hydrogel exhibited anti-biofouling properties. In the platelet adhesion experiments, fewer platelets adhered onto the surface of the zwitterionic hydrogel-coated heart valves, which was

attributed to the anti-biofouling ability of the zwitterion hydrogel. The cytotoxicity experiment and hemolysis rate experiment showed that the zwitterionic hydrogel-coated heart valves were not toxic to HUVECs and showed a hemolysis rate of less than 5%, which indicated that they had improved hemocompatibility.

Re-endothelialization is crucial to improve the hemocompatibility and stability of cardiovascular implants. The layer of endothelial cells plays an important role in the cardiovascular system in antithrombotic and antiproliferative properties. Adhesion and aggregation of platelets and leucocytes can lead to potential inflammation and thrombi [25,26]. However, a previous study showed that cytotoxicity from glutaraldehyde can result in endothelial cell death, thus leading to deficient re-endothelialization of bioprosthetic heart valves [32]. In this study, VEGF released from hydrogel can attract HUVECs to immigrate towards the heart valve surface and promote the proliferation of the adhered HUVECs to enhance the re-endothelialization potential of the heart valves. Because of the antibiofouling of zwitterionic hydrogel-coated heart valves, endothelial cells rarely adhere to their surface. As shown in the results of fluorescence microscopy and CCK-8 cell viability quantification, fewer HUVECs were observed to adhere to the surface of the zwitterionic hydrogel-coated heart valves than the zwitterionic hydrogel-coated heart valves loaded with VEGF. However, significant difference in cell number was observed between the treatment group PEGDA-MPC-DHVs and the PEGDA-MPC-DHVs@VEGF in the 3 days and 5 days, which might attribute to the effect of promoting proliferation of HUVECs [40]. All the results indicate that VEGF promotes HUVEC adhesion and proliferation onto the surface of heart valves, which is consistent with the previous hypothesis. Moreover, the adhesion of endothelial cells on the PEGDA-MPC-DHVs@VEGF might attribute to the cell adhesion sites, such as RGD in the extracellular matrix of natural heart valves [21].

Immune/inflammatory response are reported to be associated with structural valve deterioration. After implantation of prosthetic heart valves, an immune response is inevitable and is considered closely related to deterioration and calcification [16,54]. The excessive or chronic inflammation response to implanted heart valve may be adverse and undesired. Studies have found that monocytes in inflammatory reactions can drive the degradation of extracellular matrix of implanted heart valve scaffolds while macrophages can release proteolytic enzymes such as matrix metalloproteinase (MMP) and plasmin, leading to ECM degradation and stratification [55,56]. In addition, macrophages can also secrete calcium binding proteins such as osteopontin and osteopontin to promote calcification of the bioprosthetic heart valve [57]. However, previous studies have found the macrophage such as M2 macrophages plays a positive role in repair and regeneration process by supporting and activating stem/progenitor cells, clearing damaged tissue, remodeling extracellular matrix to prepare scaffolding for regeneration and promoting angiogenesis, which indicates that inflammation might have a positive effect on repair and regeneration [58,59]. Therefore, immune/inflammatory response have both beneficial and adverse aspects. In our study, heart valve samples were implanted subcutaneously into rats to evaluate the immune response, and T cells and macrophages were evaluated by immunohistochemical staining marked by CD3 and F4/80 antibodies, respectively. The PEGDA-MPC-DHVs and PEGDA-MPC-DHVs@VEGF exhibited less T-cell and macrophage infiltration in the heart valve tissue than the Glu-DHVs, which indicated that zwitterionic hydrogel coating can inhibit the infiltration of inflammatory cells in some extent, thus decreasing the immune response in the early stage. And the stratification of collagen can be observed in the Glu-DHVs, which indicates that severe and excessive immune/inflammatory response led to structural valve deterioration. However, there was still T-cell and macrophage infiltration into the heart valve tissues where the coated hydrogel had degenerated. This infiltration of immune cells might result from antigen exposure after degeneration of the hydrogel. Therefore, the property of decreasing immune response needs to be verified by further experiments.

Calcification accounts for the dysfunction of heart valves, which limits the lifespan of prosthetic heart valves [60]. In our study, alizarin red staining and ICP-OES were used to evaluate the calcification of the heart valve after 30 days of subcutaneous implantation. As these results showed, the Glu-DHVs exhibited the most calcification of the four groups, while less calcification deposition was observed in the zwitterionic hydrogel-coated heart valves, which indicated that the anti-calcification effect might be due to the hydrogel coating. A previous study showed that the anti-calcification property of zwitterionic hydrogels with a molecular network had steric and electrostatic obstruction, which can hinder the permeation of calcium [61]. However, the quantification of calcification deposition in the Glu-DHV group was lower than that in a previous study [39,62]. Multiple factors, such as the concentration of glutaraldehyde and implantation duration can affect the degree of calcification of glutaraldehyde-crosslinked bioprosthetic heart valves after implantation. Increased concentrations of glutaraldehyde and longer implantation times can lead to more calcification of bioprosthetic heart valves [17,62].

5. Limitations

The limitations of our study are as follows: first, the VEGF loading strategy by one-layer hydrogel might have some drawbacks, such as a limited amount of VEGF loading and rapid release of VEGF. The rapid released of VEGF may be detrimental to its long-term effect of promoting the adhesion and proliferation of endothelial cells. Further studies are needed to achieve a slow release of VEGF in the hybrid heart valves. Secondly, the immune response cannot be completely restrained in hybrid hydrogel-coated heart valves. Some inflammatory cells, such as microphages, can still be observed to infiltrate into hybrid hydrogel-coated heart valves. Therefore, a strategy using only zwitterion hydrogels to suppress the immune response seems limited. Further studies and anti-immune response strategies, such as the utilization of immunosuppressor, need to be developed to improve the biocompatibility of prosthetic heart valves. Moreover, the stability and durability of the seeded layer of endothelial cells is unknown. And it is unknown whether the seeded endothelial cells grow firmly on the valve surface. Maybe, it is a challenge to maintain the re-endothelialization under bloodstream, especially under high shear stress in physiological situation and further studies are needed to verify it.

6. Conclusion

In this study, hydrophilic PEGDA and zwitterionic MPC were used to coat heart valves, and the PEGDA-MPC-DHVs exhibited excellent hemocompatibility properties. The VEGF-loaded PEGDA-MPC-DHVs exhibited improved re-endothelialization potential, reduced calcification, and a mitigated immune response compared with the Glu-DHVs. In conclusion, the PEGDA-MPC-DHVs@VEGF might be a promising and alternative prosthetic heart valve for heart valve replacement in the future.

Credit authors statement

Qi Tong: Conceptualization, Methodology, Investigation, Software, Validation, Data curation, Formal analysis, Writing – original draft, Visualization; Ao Sun: Conceptualization, Methodology, Validation, Data curation, Formal analysis, Writing – review & editing; Zhengjie Wang: Formal analysis, Resources, Writing – review & editing, Visualization; Tao Li: Software, Resources, Writing – review & editing; Xinye He: Conceptualization, Methodology, Resources, Visualization; Yongjun Qian: Conceptualization, Writing – review & editing, Supervision, Project administration, Funding acquisition, Zhiyong Qian: Conceptualization, Writing – review & editing, Supervision, Project administration, Funding acquisition.

Declaration of competing interest

The authors declare that they have no known competing financial interests or personal relationships that could have appeared to influence the work reported in this paper.

Data availability

The authors do not have permission to share data.

Acknowledgements

This work was funded by the Scientific Research Project of National Clinical Research Center for Geriatrics, West China Hospital, Sichuan University (No. Z2018B19), National Natural Science Fund (Nos. NSFC U21A20417, 31930067), and 1-3-5 project for disciplines of excellence—Clinical Research Incubation Project, West China Hospital, Sichuan University (No. 2019HXFH029), and the Major Science and Technology Project of Sichuan Province, China (No. 2021YFS0121), the Science and Technology Project of Sichuan Province Health Commission, China (No. 21PJ035).

Appendix A. Supplementary data

Supplementary data to this article can be found online at <https://doi.org/10.1016/j.mtbio.2022.100459>.

References

- [1] E.S. Fioretta, P.E. Dijkman, M.Y. Emmert, S.P. Hoerstrup, The future of heart valve replacement: recent developments and translational challenges for heart valve tissue engineering, *J Tissue Eng Regen Med* 12 (1) (2018) e323–e335, <https://doi.org/10.1002/term.2326>.
- [2] E.S. Fioretta, S.E. Motta, V. Lintas, S. Loerakker, K.K. Parker, F.P.T. Baaijens, V. Falk, S.P. Hoerstrup, M.Y. Emmert, Next-generation tissue-engineered heart valves with repair, remodelling and regeneration capacity, *Nat. Rev. Cardiol.* 18 (2) (2021) 92–116, <https://doi.org/10.1038/s41569-020-0422-8>.
- [3] J.C. Sun, M.J. Davidson, A. Lamy, J.W. Eikelboom, Antithrombotic management of patients with prosthetic heart valves: current evidence and future trends, *Lancet* 374 (9689) (2009) 565–576, [https://doi.org/10.1016/S0140-6736\(09\)60780-7](https://doi.org/10.1016/S0140-6736(09)60780-7).
- [4] D. Mohanany, M. Aljadah, A.A.H. Smith, J.F. Haines, S. Patel, P. Villablanca, H. Ramakrishna, The 2020 ACC/AHA guidelines for management of patients with valvular heart disease: highlights and perioperative implications, *J. Cardiothorac. Vasc. Anesth.* 36 (5) (2022) 1467–1476, <https://doi.org/10.1053/j.jvca.2021.04.013>.
- [5] G.Y. Guo, L.H. Jin, B.G. Wu, H.Y. He, F. Yang, L.P. Xu, Y. Lei, Y.B. Wang, A method for simultaneously crosslinking and functionalizing extracellular matrix-based biomaterials as bioprosthetic heart valves with enhanced endothelialization and reduced inflammation, *Acta Biomater.* 119 (2021) 89–100, <https://doi.org/10.1016/j.actbio.2020.10.029>.
- [6] D.F. Williams, D. Bezuidenhout, J. de Villiers, P. Human, P. Zilla, Long-term stability and biocompatibility of pericardial bioprosthetic heart valves, *Front Cardiovasc. Med.* 8 (2021), 728577, <https://doi.org/10.3389/fcvm.2021.728577>.
- [7] S. Nakatani, Subclinical leaflet thrombosis after transcatheter aortic valve implantation, *Heart* 103 (24) (2017) 1942–1946, <https://doi.org/10.1136/heartjnl-2017-311818>.
- [8] M. Bogyi, R.E. Scherthaner, C. Loewe, G.M. Gager, A.M. Dizdarevic, C. Kronberger, M. Postula, J. Legutko, P. Velagapudi, C. Hengstenberg, J.M. Siller-Matula, Subclinical leaflet thrombosis after transcatheter aortic valve replacement: a meta-analysis, *JACC Cardiovasc. Interv.* 14 (24) (2021) 2643–2656, <https://doi.org/10.1016/j.jcin.2021.09.019>.
- [9] M. Della Barbera, E. Pettenazzo, U. Livi, D. Mangino, G. Gerosa, T. Bottio, C. Basso, M. Valente, G. Thiene, Structural valve deterioration and mode of failure of stentless bioprosthetic valves, *Cardiovasc. Pathol.* 51 (2021), 107301, <https://doi.org/10.1016/j.carpath.2020.107301>.
- [10] M. Marro, A.P. Kossar, Y. Xue, A. Frasca, R.J. Levy, G. Ferrari, Noncalcific mechanisms of bioprosthetic structural valve degeneration, *J. Am. Heart Assoc.* 10 (3) (2021), e018921, <https://doi.org/10.1161/JAHA.120.018921>.
- [11] S. Wen, Y. Zhou, W.Y. Yim, S. Wang, L. Xu, J. Shi, W. Qiao, N. Dong, Mechanisms and drug therapies of bioprosthetic heart valve calcification, *Front. Pharmacol.* 13 (2022), 909801, <https://doi.org/10.3389/fphar.2022.909801>.
- [12] S.R. Tuladhar, S. Mulderrig, M. Della Barbera, L. Vedovelli, D. Bottigliengo, C. Tessari, S. Jockenhoevel, D. Gregori, G. Thiene, S. Korossis, P. Mela, L. Iop, G. Gerosa, Bioengineered percutaneous heart valves for transcatheter aortic valve replacement: a comparative evaluation of decellularised bovine and porcine pericardium, *Mater Sci. Eng. C Mater. Biol. Appl.* 123 (2021), 111936, <https://doi.org/10.1016/j.msec.2021.111936>.
- [13] S.J. Head, M. Celik, A.P. Kappetein, Mechanical versus bioprosthetic aortic valve replacement, *Eur. Heart J.* 38 (28) (2017) 2183–2191, <https://doi.org/10.1093/eurheartj/ehx141>.
- [14] Y. Luo, S. Huang, L. Ma, A novel detergent-based decellularization combined with carbodiimide crosslinking for improving anti-calcification of bioprosthetic heart valve, *Biomed. Mater.* 16 (4) (2021), <https://doi.org/10.1088/1748-605X/ac0088>.
- [15] P. Human, C. Ofogebu, H. Ilsley, D. Bezuidenhout, J. de Villiers, D.F. Williams, P. Zilla, Decellularization and engineered crosslinking: a promising dual approach towards bioprosthetic heart valve longevity, *Eur. J. Cardio. Thorac. Surg.* 58 (6) (2020) 1192–1200, <https://doi.org/10.1093/ejcts/ezaa257>.
- [16] R.A. Manji, L.F. Zhu, N.K. Nijjar, D.C. Rayner, G.S. Korbutt, T.A. Churchill, R.V. Rajotte, A. Koshal, D.B. Ross, Glutaraldehyde-fixed bioprosthetic heart valve conduits calcify and fail from xenograft rejection, *Circulation* 114 (4) (2006) 318–327, <https://doi.org/10.1161/Circulationaha.105.549311>.
- [17] P. Sinha, D. Zurakowski, T.K.S. Kumar, D.C. He, C. Rossi, R.A. Jonas, Effects of glutaraldehyde concentration, pretreatment time, and type of tissue (porcine versus bovine) on postimplantation calcification, *J. Thorac. Cardio. Sur.* 143 (1) (2012) 224–227, <https://doi.org/10.1016/j.jtcvs.2011.09.043>.
- [18] A.F. Badria, P.G. Koutsoukos, D. Mavrilas, Decellularized tissue-engineered heart valves calcification: what do animal and clinical studies tell us? *J. Mater. Sci. Mater. Med.* 31 (12) (2020) 132, <https://doi.org/10.1007/s10856-020-06462-x>.
- [19] Z. Sun, J. Liu, X. Wang, H. Jing, B. Li, D. Kong, X. Leng, Z. Wang, Epoxy chitosan-crosslinked acellular bovine pericardium with improved anti-calcification and biological properties, *ACS Appl. Bio Mater.* 3 (4) (2020) 2275–2283, <https://doi.org/10.1021/acsabm.0c00067>.
- [20] C. Liu, W. Qiao, H. Cao, J. Dai, F. Li, J. Shi, N. Dong, A riboflavin-ultraviolet light A-crosslinked decellularized heart valve for improved biomechanical properties, stability, and biocompatibility, *Biomater. Sci.* 8 (9) (2020) 2549–2563, <https://doi.org/10.1039/c9bm01956a>.
- [21] F. Yang, L.P. Xu, D.J. Kuang, Y. Ge, G.Y. Guo, Y.B. Wang, Polyzwitterion-crosslinked hybrid tissue with antithrombogenicity, endothelialization, anticalcification properties, *Chem. Eng. J.* 410 (2021), <https://doi.org/10.1016/j.cej.2020.128244>.
- [22] Y. Luo, S.Y. Huang, L. Ma, Zwitterionic hydrogel-coated heart valves with improved endothelialization and anti-calcification properties, *Mat Sci. Eng. C-Mater.* 128 (2021), <https://doi.org/10.1016/j.msec.2021.112329>.
- [23] L. Zhang, T. Li, Y. Yu, K. Shi, Z. Bei, Y. Qian, Z. Qian, An injectable conductive hydrogel restores electrical transmission at myocardial infarct site to preserve cardiac function and enhance repair, *Bioact. Mater.* 20 (2022) 339–354, <https://doi.org/10.1016/j.bioactmat.2022.06.001>.
- [24] K. Ding, C. Zheng, X. Huang, S. Zhang, M. Li, Y. Lei, Y. Wang, A PEGylation method of fabricating bioprosthetic heart valves based on glutaraldehyde and 2-amino-4-pentenoic acid co-crosslinking with improved antithrombogenicity and cytocompatibility, *Acta Biomater.* 144 (2022) 279–291, <https://doi.org/10.1016/j.actbio.2022.03.026>.
- [25] S. Jana, Endothelialization of cardiovascular devices, *Acta Biomater.* 99 (2019) 53–71, <https://doi.org/10.1016/j.actbio.2019.08.042>.
- [26] T. Liu, S. Liu, K. Zhang, J. Chen, N. Huang, Endothelialization of implanted cardiovascular biomaterial surfaces: the development from in vitro to in vivo, *J. Biomed. Mater. Res.* 102 (10) (2014) 3754–3772, <https://doi.org/10.1002/jbm.a.35025>.
- [27] J.M. Reimer, Z.H. Syedain, B.H. Haynie, R.T. Tranquillo, Pediatric tubular pulmonary heart valve from decellularized engineered tissue tubes, *Biomaterials* 62 (2015) 88–94, <https://doi.org/10.1016/j.biomaterials.2015.05.009>.
- [28] G. Guo, L. Jin, W. Jin, L. Chen, Y. Lei, Y. Wang, Radical polymerization-crosslinking method for improving extracellular matrix stability in bioprosthetic heart valves with reduced potential for calcification and inflammatory response, *Acta Biomater.* 82 (2018) 44–55, <https://doi.org/10.1016/j.actbio.2018.10.017>.
- [29] B. Wu, C. Zheng, K. Ding, X. Huang, M. Li, S. Zhang, Y. Lei, Y. Guo, Y. Wang, Cross-linking porcine pericardium by 3,4-dihydroxybenzaldehyde: a novel method to improve the biocompatibility of bioprosthetic valve, *Biomacromolecules* 22 (2) (2021) 823–836, <https://doi.org/10.1021/acs.biomac.0c01554>.
- [30] J. Liu, H. Jing, Y. Qin, B. Li, Z. Sun, D. Kong, X. Leng, Z. Wang, Nonglutaraldehyde fixation for the shell decellularized bovine pericardium in anticalcification cardiac valve applications, *ACS Biomater. Sci. Eng.* 5 (3) (2019) 1452–1461, <https://doi.org/10.1021/acsbiomaterials.8b01311>.
- [31] F. Yang, H.Y. He, L.P. Xu, L.H. Jin, G.Y. Guo, Y.B. Wang, Inorganic-polymerization crosslinked tissue-siloxane hybrid as potential biomaterial for bioprosthetic heart valves, *J. Biomed. Mater. Res.* 109 (5) (2021) 754–765, <https://doi.org/10.1002/jbm.a.37061>.
- [32] M. Lopez-Moya, P. Melgar-Lesmes, K. Kolandaivelu, J.M. de la Torre Hernandez, E.R. Edelman, M. Balcells, Optimizing glutaraldehyde-fixed tissue heart valves with chondroitin sulfate hydrogel for endothelialization and shielding against deterioration, *Biomacromolecules* 19 (4) (2018) 1234–1244, <https://doi.org/10.1021/acs.biomac.8b00077>.
- [33] X. Wang, K.L. Wen, X. Yang, L. Li, X.X. Yu, Biocompatibility and anti-calcification of a biological artery immobilized with naturally-occurring phytic acid as the crosslinking agent, *J. Mater. Chem. B* 5 (40) (2017) 8115–8124, <https://doi.org/10.1039/c7tb02909b>.
- [34] T. Yu, W. Yang, W. Zhuang, Y. Tian, Q. Kong, X. Chen, G. Li, Y. Wang, A bioprosthetic heart valve cross-linked by a non-glutaraldehyde reagent with improved biocompatibility, endothelialization, anti-coagulation and anti-calcification properties, *J. Mater. Chem. B* 9 (19) (2021) 4031–4038, <https://doi.org/10.1039/d1tb00409c>.
- [35] D. Zhu, L. Jin, X. Wang, L. Xu, T. Liu, Combined anticalcification treatment of bovine pericardium with decellularization and hyaluronic acid derivative, *Bio Med. Mater. Eng.* 24 (1) (2014) 741–749, <https://doi.org/10.3233/BME-130862>.

- [36] S. Boroumand, S. Asadpour, A. Akbarzadeh, R. Faridi-Majidi, H. Ghanbari, Heart valve tissue engineering: an overview of heart valve decellularization processes, *Regen. Med.* 13 (1) (2018) 41–54, <https://doi.org/10.2217/rme-2017-0061>.
- [37] Y. Snyder, S. Jana, Strategies for development of decellularized heart valve scaffolds for tissue engineering, *Biomaterials* 288 (2022), 121675, <https://doi.org/10.1016/j.biomaterials.2022.121675>.
- [38] V.V. Sevostyanova, L.V. Antonova, E.A. Velikanova, V.G. Matveeva, E.O. Krivkina, T.V. Glushkova, A.V. Mironov, A.Y. Burago, L.S. Barbarash, Endothelialization of polycaprolactone vascular graft under the action of locally applied vascular endothelial growth factor, *Bull. Exp. Biol. Med.* 165 (2) (2018) 264–268, <https://doi.org/10.1007/s10517-018-4144-4>.
- [39] Y. Lei, L. Deng, Y. Tang, Q. Ning, X. Lan, Y. Wang, Hybrid pericardium with VEGF-loaded hyaluronic acid hydrogel coating to improve the biological properties of bioprosthetic heart valves, *Macromol. Biosci.* 19 (6) (2019), e1800390, <https://doi.org/10.1002/mabi.201800390>.
- [40] N. Marival, M. Morenc, M.N. Labour, A. Samotus, A. Mzyk, V. Ollivier, M. Maire, K. Jesse, K. Bassand, A. Niemiec-Cyganek, O. Haddad, M.P. Jacob, F. Chaubet, N. Charnaud, P. Wilczek, H. Hlawaty, Fucoidan/VEGF-based surface modification of decellularized pulmonary heart valve improves the antithrombotic and re-endothelialization potential of bioprostheses, *Biomaterials* 172 (2018) 14–29, <https://doi.org/10.1016/j.biomaterials.2018.01.054>.
- [41] Q. Li, Y. Bai, T. Jin, S. Wang, W. Cui, I. Stanculescu, R. Yang, H. Nie, L. Wang, X. Zhang, Bioinspired engineering of poly(ethylene glycol) hydrogels and natural protein fibers for layered heart valve constructs, *ACS Appl. Mater. Interfaces* 9 (19) (2017) 16524–16535, <https://doi.org/10.1021/acsami.7b03281>.
- [42] V.V. Ganesan, M. Dhanasekaran, N. Thangavel, A. Dhathathreyan, Elastic compliance of fibrillar assemblies in type I collagen, *Biophys. Chem.* 240 (2018) 15–24, <https://doi.org/10.1016/j.bpc.2018.05.007>.
- [43] I.H. Jaffer, J.I. Weitz, The blood compatibility challenge. Part 1: blood-contacting medical devices: the scope of the problem, *Acta Biomater.* 94 (2019) 2–10, <https://doi.org/10.1016/j.actbio.2019.06.021>.
- [44] G.D. Dangas, J.I. Weitz, G. Giustino, R. Makkar, R. Mehran, Prosthetic heart valve thrombosis, *J. Am. Coll. Cardiol.* 68 (24) (2016) 2670–2689, <https://doi.org/10.1016/j.jacc.2016.09.958>.
- [45] J. Zhang, L. Chen, L. Chen, S. Qian, X. Mou, J. Feng, Highly antifouling, biocompatible and tough double network hydrogel based on carboxybetaine-type zwitterionic polymer and alginate, *Carbohydr. Polym.* 257 (2021), 117627, <https://doi.org/10.1016/j.carbpol.2021.117627>.
- [46] Y. Xie, L. Chen, X. Zhang, S. Chen, M. Zhang, W. Zhao, S. Sun, C. Zhao, Integrating zwitterionic polymer and Ag nanoparticles on polymeric membrane surface to prepare antifouling and bactericidal surface via Schiff-based layer-by-layer assembly, *J. Colloid Interface Sci.* 510 (2018) 308–317, <https://doi.org/10.1016/j.jcis.2017.09.071>.
- [47] Y. Wang, X. Cao, M. Ma, W. Lu, B. Zhang, Y. Guo, A GelMA-PEGDA-nHA composite hydrogel for bone tissue engineering, *Materials* 13 (17) (2020), <https://doi.org/10.3390/ma13173735>.
- [48] E. Secret, S.J. Kelly, K.E. Crannell, J.S. Andrew, Enzyme-responsive hydrogel microparticles for pulmonary drug delivery, *ACS Appl. Mater. Interfaces* 6 (13) (2014) 10313–10321, <https://doi.org/10.1021/am501754s>.
- [49] Z.X. Huang, H. Ghasemi, Hydrophilic polymer-based anti-biofouling coatings: preparation, mechanism, and durability, *Adv. Colloid Interfac.* 284 (2020), <https://doi.org/10.1016/j.cis.2020.102264>.
- [50] M. Li, B. Zhuang, J. Yu, Functional zwitterionic polymers on surface: structures and applications, *Chem. Asian J.* 15 (14) (2020) 2060–2075, <https://doi.org/10.1002/asia.202000547>.
- [51] A.B. Asha, Y. Chen, R. Narain, Bioinspired dopamine and zwitterionic polymers for non-fouling surface engineering, *Chem. Soc. Rev.* 50 (20) (2021) 11668–11683, <https://doi.org/10.1039/d1cs00658d>.
- [52] C.A. Labarrere, A.E. Dabiri, G.S. Kassab, Thrombogenic and inflammatory reactions to biomaterials in medical devices, *Front. Bioeng. Biotechnol.* 8 (2020) 123, <https://doi.org/10.3389/fbioe.2020.00123>.
- [53] G. Guo, W. Jin, L. Jin, L. Chen, Y. Lei, Y. Wang, Hydrogel hybrid porcine pericardium for the fabrication of a pre-mounted TAVI valve with improved biocompatibility, *J. Mater. Chem. B* 7 (9) (2019) 1427–1434, <https://doi.org/10.1039/c8tb02565g>.
- [54] S.J. Bozso, R. El-Andari, D. Al-Adra, M.C. Moon, D.H. Freed, J. Nagendran, J. Nagendran, A review of the immune response stimulated by xenogenic tissue heart valves, *Scand. J. Immunol.* 93 (4) (2021), e13018, <https://doi.org/10.1111/sji.13018>.
- [55] T. Sakae, H. Nakaoka, F. Shikata, J. Aono, M. Kurata, T. Uetani, M. Hamaguchi, A. Kojima, S. Uchita, T. Yasugi, H. Higashi, J. Suzuki, S. Ikeda, J. Higaki, S. Higashiyama, H. Izutani, Biochemical and histological evidence of deteriorated bioprosthetic valve leaflets: the accumulation of fibrinogen and plasminogen, *Biol. Open* 7 (8) (2018), <https://doi.org/10.1242/bio.034009>.
- [56] S. Sprangers, V. Everts, Molecular pathways of cell-mediated degradation of fibrillar collagen, *Matrix Biol.* 75–76 (2019) 190–200, <https://doi.org/10.1016/j.matbio.2017.11.008>.
- [57] Y.S. Zhu, Y. Gu, C. Jiang, L. Chen, Osteonectin regulates the extracellular matrix mineralization of osteoblasts through P38 signaling pathway, *J. Cell. Physiol.* 235 (3) (2020) 2220–2231, <https://doi.org/10.1002/jcp.29131>.
- [58] Y. Oishi, I. Manabe, Macrophages in inflammation, repair and regeneration, *Int. Immunol.* 30 (11) (2018) 511–528, <https://doi.org/10.1093/intimm/dxy054>.
- [59] C.D. Mills, M1 and M2 macrophages: oracles of health and disease, *Crit. Rev. Immunol.* 32 (6) (2012) 463–488, <https://doi.org/10.1615/critrevimmunol.v32.i6.10>.
- [60] S. Lee, R.J. Levy, A.J. Christian, S.L. Hazen, N.E. Frick, E.K. Lai, J.B. Grau, J.E. Bavaria, G. Ferrari, Calcification and oxidative modifications are associated with progressive bioprosthetic heart valve dysfunction, *J. Am. Heart Assoc.* 6 (5) (2017), <https://doi.org/10.1161/JAHA.117.005648>.
- [61] F. Guo, Y.N. Liu, K. Jiao, R. Yang, M.X. Hou, X. Zhang, Artificial heart valves with balanced charged networks exhibiting anti-calcification properties, *ACS Appl. Bio Mater.* 3 (2) (2020) 838–847, <https://doi.org/10.1021/acsabm.9b00902>.
- [62] C. Hu, R.F. Luo, Y.B. Wang, Heart valves cross-linked with erythrocyte membrane drug-loaded nanoparticles as a biomimetic strategy for anti-coagulation, anti-inflammation, anti-calcification, and endothelialization, *ACS Appl. Mater. Inter.* 12 (37) (2020) 41113–41126, <https://doi.org/10.1021/acsami.0c12688>.